Molecular simulation of Dissolved Inorganic Carbons for Underground Brine CO2 Sequestrations
Project Number:DE-FE0002057

California Institute of Technology

Professor William A. Goddard III

1-2pm EST, Tuesday February 23, 2010

Dawn Marie Deel, PMP, Project Manager
National Energy Technology Laboratory
Environment and Climate Division
PO Box 880
Morgantown, WV 26507-0880
Office: 304-285-4133; Cell: 304-807-4917
dawn.deel@netl.doe.gov

Introduction

For Monitoring, Verification and Accounting (MVA) of CO2 sequestration. need to measure the Dissolved Inorganic Carbons (DIC) in underground brine water at *higher sensitivity, lower cost, in situ, at higher frequency and over long period of time*

Quantum Cascade Lasers (QCL) could provide Mid-IR spectroscopic measurement that could provide higher sensitivity of DIC measurement, to "quantify and resolve at high sensitivity over an extended spatial scale; improve the reliability of next-generation detection and sensing technologies; and quantify the mass of sequestered CO2, over its volume (both depth and lateral extent) and as a function of time "(technical Area #2 of the FOA).

To interpret the results of such studies, need to predict how the Mid-IR spectra for CO2 (aq, or dissolved) and HCO3- change as a function of pressure, pH, temperature and salinity.

Objectives

Use first principles QM and ReaxFF to predict the MIR spectra of DIC species in water.

Determine how the MIR spectra change with external conditions (temperature, pressure, salinity).

Determine the acidity changes as a result of pressure, temperature and the presence of supercritical CO_2 during underground brine water carbon sequestration process.

Provide graduate students and scientists professional training in molecular simulation to prepare them for the applications of the acquired knowledge for carbon sequestration.

Specific Technical objectives

Simulation and identification of the Mid-IR absorption features of CO2 (aq) and HCO3-;

Simulation of the Mid-IR absorption spectral changes as the pressure, pH, temperature, and salinity change;

Calculation of the resulting pH and equilibrium constants for the dissolved inorganic carbon species in brine waters under high pressure, high temperature, and high CO2 concentration conditions;

Thus illustrate chemistry reaction pathways for CO2 sequestration in underground brine water and rock cap reservoirs.

Project Funding

		Year 1	Year 2	Year 3		TOTAL
SALARIES						
Principal Investigator- WAG	0.01	$ 2,000	$ 2,000	$ 2,000		$ 6,000
Graduate Students (2 each with h	1.00	$ 25,500	$ 25,500	$ 25,500		$ 76,500
Undergraduate	2.00	$ 12,000	$ 12,000	$ 12,000		$ 36,000
Total salaries		$ 39,500	$ 39,500	$ 39,500		$ 118,500
Staff benefits (excluding students)	**25.0%**	$ 500	$ 500	$ 500		$ 1,500
Tuition Remission Allocation	**63.5%**	$ 16,193	$ 16,193	$ 16,193		$ 48,578
Materials and Supplies		$ 2,233	$ 2,233	$ 2,233		$ 6,699
Publications		$ 1,000	$ 1,000	$ 1,000		$ 3,000
Computer Services		$ 7,500	$ 7,500	$ 7,500		$ 22,500
Travel		$ 1,000	$ 1,000	$ 1,000		$ 3,000
Total Direct Costs		$ 67,926	$ 67,926	$ 67,926		$ 203,777
Indirect Costs @ 62%		$ 32,074	$ 32,074	$ 32,074		$ 96,223
(Excludes Tuition benefit, equipment, Subcontractor >25k)						
Grand TOTAL		**$ 100,000**	**$ 100,000**	**$ 100,000**		**$ 300,000**
Indirect Cost Base		$ 51,733	$ 51,733	$ 51,733		$ 155,199
		$ 100,000	$ 100,000	$ 100,000		$ 300,000

Tasks, Phase I (1-12 months)

Survey of DIC species MIR spectra and change with water conditions

Task 1.0 – DFT simulation of DIC species

Subtask 1.1 Verification of DFT simulation through CO2 dissolved Mid-IR spectra

We proposed to perform QM electronic structure calculation on solvated CO2, HCO3- and CO32- species, comparing and adjusting the calculated vibrational IR frequencies to those of experiment.

This would give us confidence that we are describing the physical system.

Status – *A. Vibrational Spectra of Gas-Phase $C0_2$ and H_2O*

DFT QM electronic structure calculations were performed, using the Jaguar 7.0 QM package and the augmented split-valence double (aug-cc-pVDZ) and triple (aug-cc-pVTZ) zeta basis set of Dunning and coworkers.

We tested the accuracy of the B3LYP, X3LYP, M06, M06-2X and M06-HF DFT functionals in predicting the vibrational frequencies of CO2 and H2O in the gas phase and in implicit solvation, using the PDF module in the Jaguar 7.0 package.

All functionals gave similar performance (within 5 cm-1 of each other).

We list the frequencies of the best performer (B3LYP) in Table 1.

Both basis sets show reasonable agreement with experiment, with the double zeta predicting the frequencies more accurately on average.

Frequencies H_2O, CO_2

	Frequencies (cm^{-1})			
	Experiment	**aug-cc-pVTZ**	**aug-cc-pVDZ**	**assignment**
H_2O				
v2	1594.7	1628.4	1622.3	symmetric bending
v1	3657.1	3821.9	3803.3	symmetric stretch
v3	3756	3947.7	3937.5	antisymmetric stretch
CO_2				
v2	667	659	655.5	degenerate bending OCO
v1	1388	1325.8	1305.4	symmetric stretch OC
v3	2349	2401.4	2379.2	antisymmetric stretch OC

This provides a calibration for the accuracy of DFT

In practice we will use these scaling parameters to adjust predicted results for the aqueous phases under various conditions

Status B. Vibrational Spectra of the CO2-H2O dimer

We map the four dimensional potential energy surface (PES) of the CO_2-H_2O dimer (Figure 1).

We find a quadruply degenerate minimum, with the water molecule forming a single hydrogen bond with the CO_2.

The calculated vibrational spectra show the characteristic red shift of 5 cm-1 in the vibrational modes arising from this hydrogen bond.

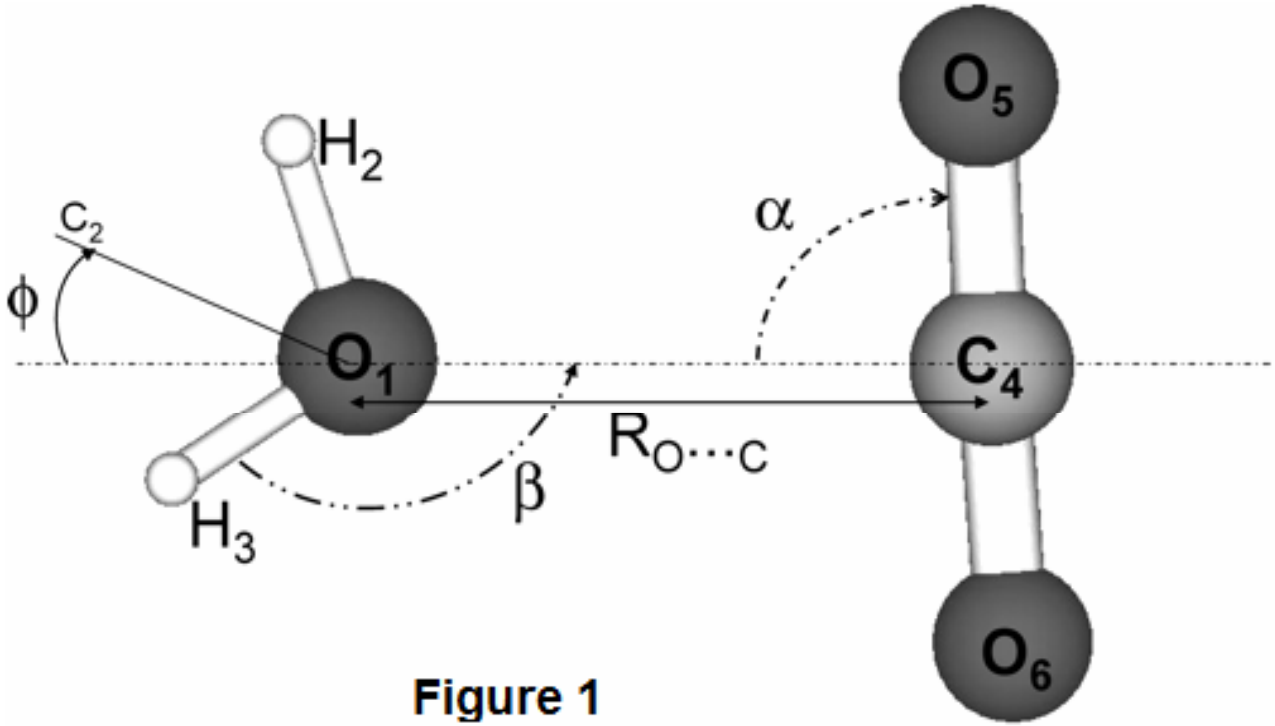

Figure 1

	Frequencies (cm^{-1})		
	aug-cc-pVTZ	**aug-cc-pVDZ**	**assignment**
v21	648.8	646.6	in-plane bending
v22	662.6	657.8	out-of-plane bending
v1(CO)	1328.6	1308.7	symmetric stretch OC
v2(HOH)	1626.5	1619.2	symmetric bending
v3(CO)	2404.4	2383.2	antisymmetric stretch OC
v1(OH)	3818.5	3800.2	symmetric stretch
v3(OH)	3944.6	3935.3	antisymmetric stretch

Subtask 1.2 DFT simulation for HCO3- Mid-IR spectra

DFT studies of the vibrational spectra of various species will be performed using the X3LYP26 DFT functional and the augmented polarized triple-ζ 6-311+G(2df,2p)27 basis set.

This level of theory has proved accurate in describing the hydrogen bonding and electrostatic interactions that will be dominated in these solvated systems.

<u>Status</u>

These calculations are currently being performed.

DFT simulation for HCO3- Mid-IR spectra

- We prepared clusters of CO2(H2O)x and HCO3-(H2O)x (x = 0 – 10) structures by energy minimization using the Dreiding[1] forcefield and the LAMMPS 2010 MD[2] engine. In order to ensure accurate sampling of the potential energy surface, the water molecules were placed in several random configurations for each sized cluster and the top 5 conformers (ranked by total energy) were then selected for electronic structure calculations using the Jaguar 7.5 program[3]. Geometry optimization was initially performed using the X3LYP[4] DFT functional and the augmented polarized triple-ζ 6-311+G(2df,2p)[5] basis set. The optimized gas phase geometries were then used as input to an implicit solvent calculation with the PBF module in Jaguar, using the accepted parameters of water: dielectric constant: 80.37, density: 0.99823, molecular weight: 18.02 g/mol, probe radius 1.40Å. Vibrational analysis was performed at all optimized geometries to ensure that the structures corresponded to local minimas. The optimized geometries are shown in Figure 1. All the energetics presented herein were derived from the X3LYP/6-311+G*(2df,2p) values and include the scaled zero-point energy correction.

HCO3-	n=1	n=2	n=3	n=4	n=5
	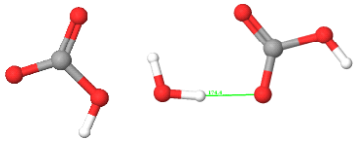	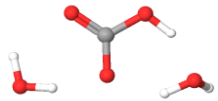	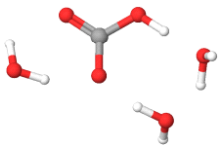	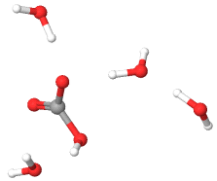	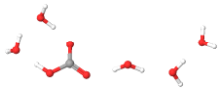
	n=6	n=7	n=8	n=9	n=10
	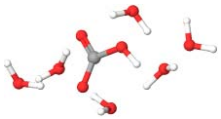	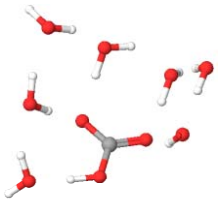	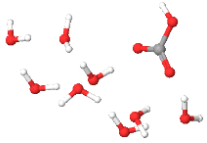	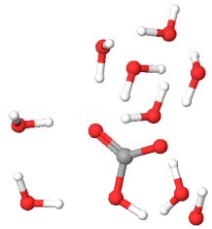	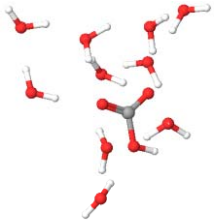
CO2	n=1	n=2	n=3	n=4	n=5
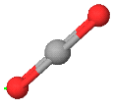	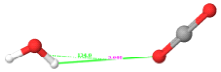	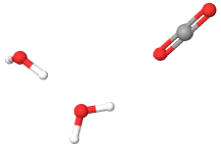	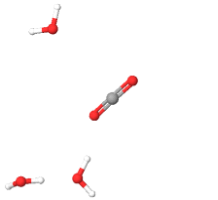	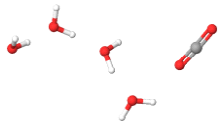	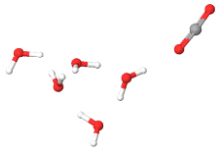
	n=6	n=7	n=8	n=9	n=10
	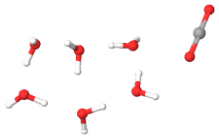	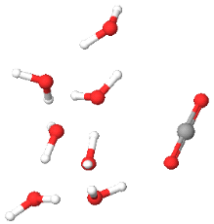	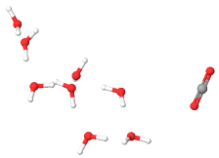	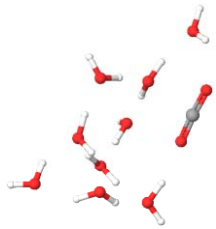	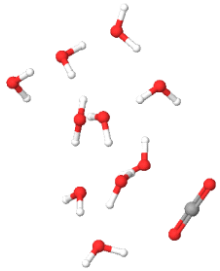

The most stable structure is found to be CO2(H2O)6 and CO2(H2O)7 (Figure 2).

Figure 2: Average water binding energy for CO2(H2O)x complexes. The minimum energy structure occur at n = 6 and n = 7.

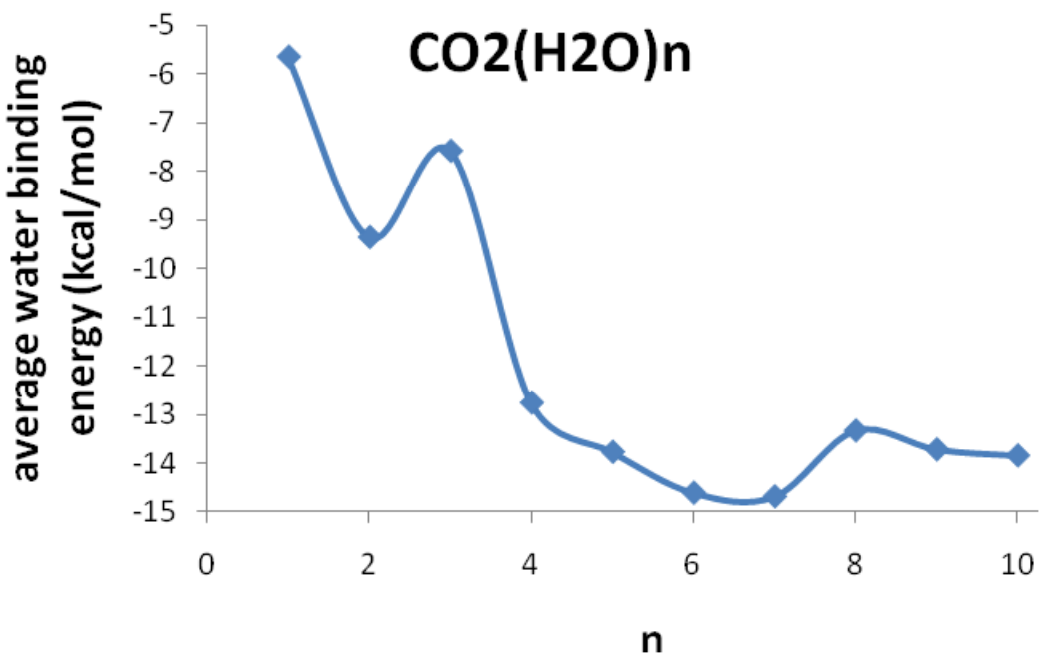

For the HCO3-(H2O)n structures, the first water molecule forms a strong hydrogen bond with the O- group (water is the h-bond donor), the second water forms a hydrogen bond with the OH group (water is the h-bond acceptor), while the third water forms a weaker h-bond with the double bonded O group. The forth forms begins a second shell by hydrogen bonding with the first water molecule. The HCO3- is completely solvated by the water shells and we although we find a minima for the HCO3-(H2O)4 conformer, the HCO3-(H2O)7 conformer and HCO3-(H2O)9 conformers are all within 0.5 kcal/mol (the accuracy of our method) (Figure 3).

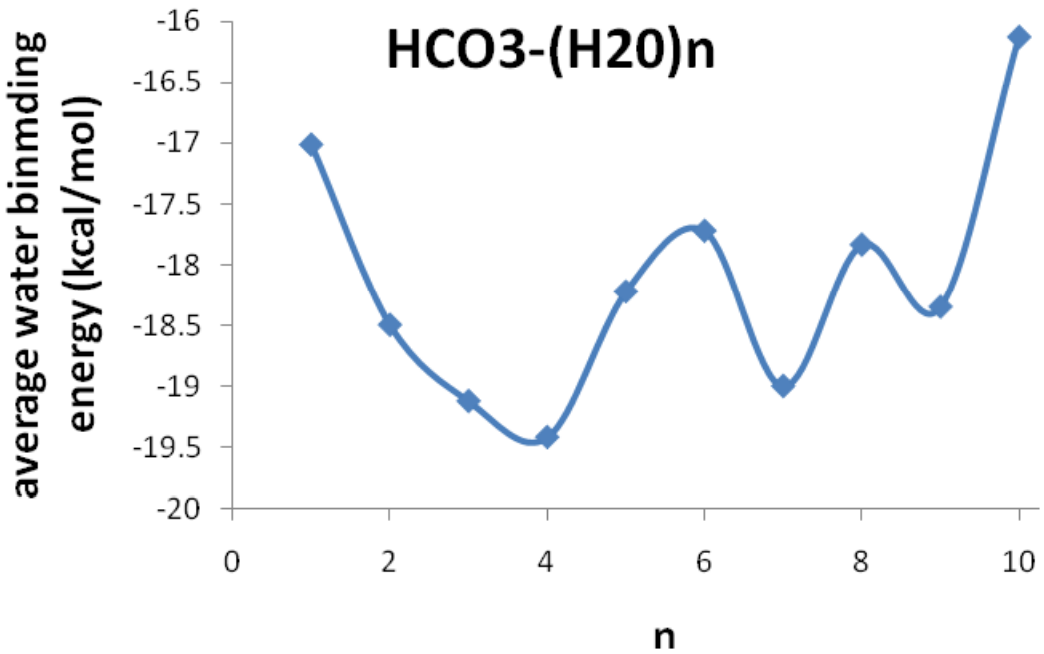

Simulated infrared spectras for the lowest energy complexes were then derived from the B3LYP/6-31G*(d,p) scaled harmonic frequencies (scaling factor: 0.9614). In table 1, we list the shift in the vibrational frequencies of the free molecules with increasing water cluster sizes.

Peak frequency (cm^{-1})	422	540	621	743	878	1160	1260	1580	1588	3668	3676
H20								H-O-H bending		H-O-H stretch	H-O-H asymmetric stretch
CO2		O-C-O bending					C-O symmetric stretch		C-O asymmetric stretch		
$HCO3^-$	C-OH rock	(538)	O-C-O bend	C-O-H bend	C-OH stretch	In-plane C-O bending	(1255)	Out of plane bending	(1590)		

Subtask 1.3 Experimental proof of the simulated spectra

The FTIR spectra for different species of CO2 when dissolved in water is measured with a Thermo Nicolet Nexus 470 FTIR equipped with a ATR module (Figure 4). CO2 species in water, i.e. CO2(aq), H2CO3, HCO3- and CO32-, are trapped in a cotton ball and then put on top of the diamond tip of the ATR module.

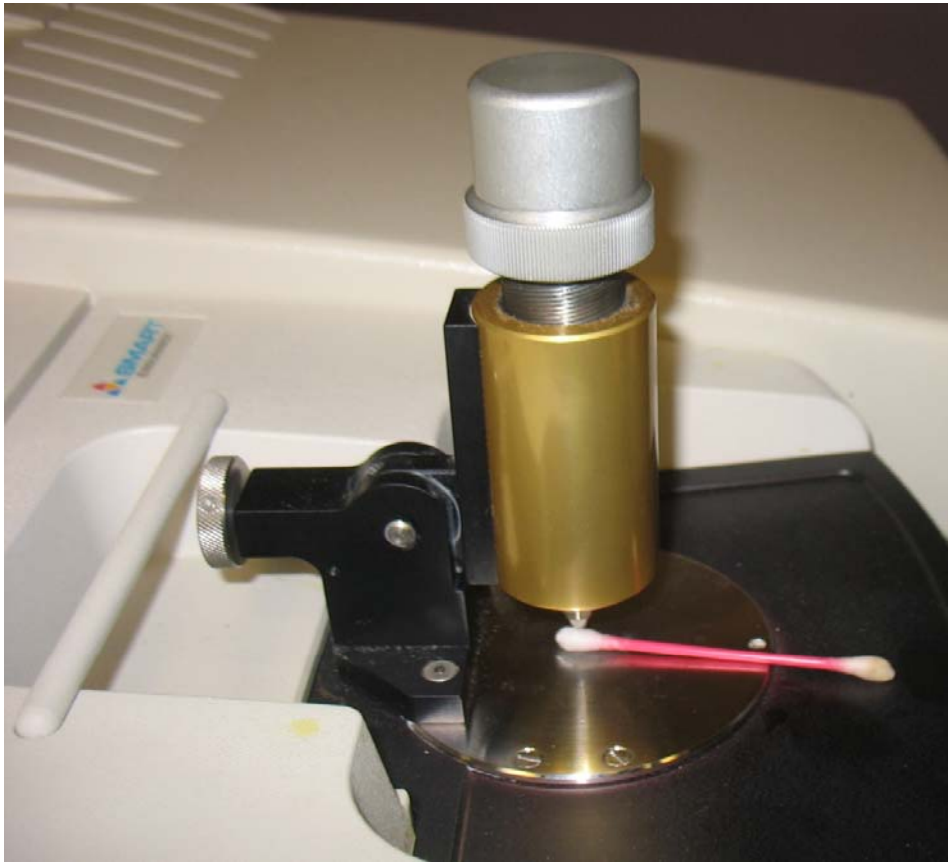

All spectra were collected with 32 averages at either 4cm-1 resolution. The concentration of the HCO3- and CO32- are prepared in test tube/vials, and then transferred to cotton ball tip, then acid is added to convert the HCO3- and CO32- into CO2(aq) and H2CO3. So, the initial concentrations of HCO3- and CO32- is accurate as prepared, while the concentration of HCO3- and CO32- along with CO2(aq) and H2CO3 are varying after HCl acid is applied.
We generated the spectra of ~~0.1M Na2CO3 with H2O background subtracted --- Blue trace; Spectra of ~0.1M KHCO3 with H2O background subtracted --- Red trace (figure 5).

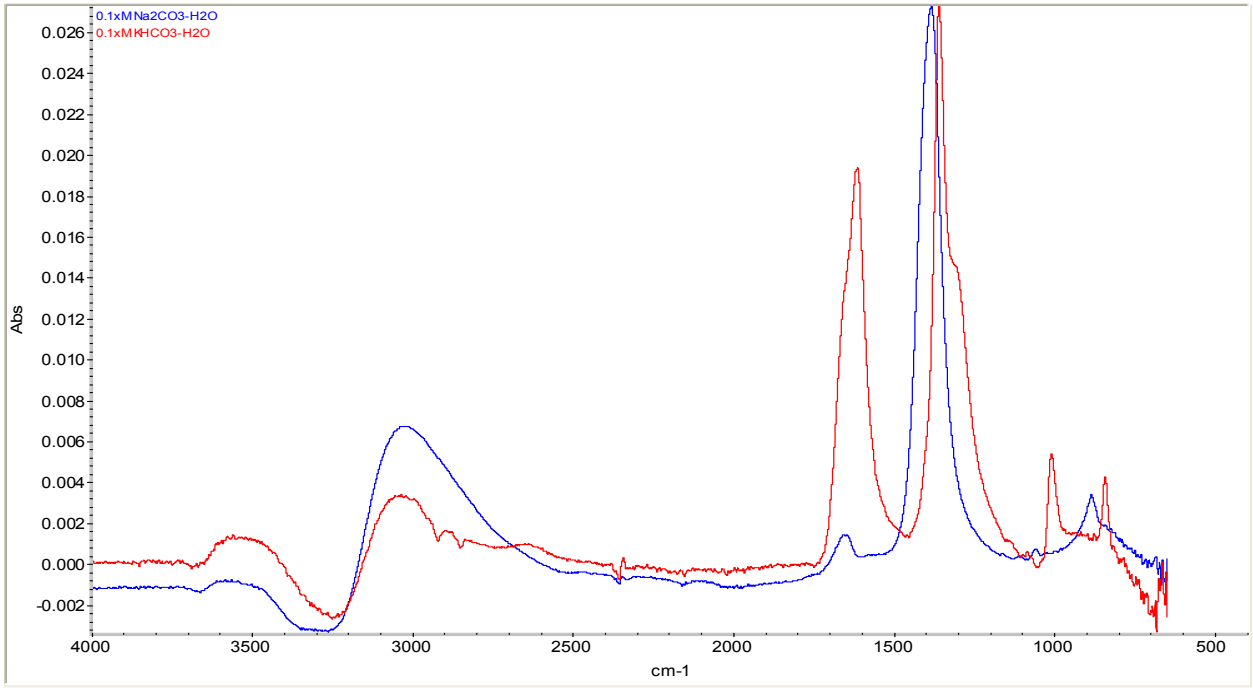

Peak Frequency	840	1010	1300	1360	1630	890	1060	1380	1680	2342
Na2CO3						ν2	ν1	ν3	?2x ν2	
KHCO3	ν8	ν5	ν4	ν3	?ν2/H2O					
CO2										??

According to our calculations, we have the following assignment of the peaks:

Thermodynamics of liquid and super-critical Co2

Entropy, heat capacity and free energy over the phase diagram using 2PT molecular dynamics

MATERIALS AND PROCESS SIMULATION CENTER,
CALIFORNIA INSTITUTE OF TECHNOLOGY, PASADENA, CA 91125

Entropy: What is it?

$$\Delta G_t = \Delta H_t - T\Delta S_t$$

Entropy:	a state variable whose change is defined for a reversible process at T where Q is the heat absorbed.
Entropy:	a measure of the amount of energy which is unavailable to do work.
Entropy:	a measure of the disorder of a system.
Entropy:	a measure of the multiplicity of a system.

$$\Delta S = \frac{Q}{T}$$

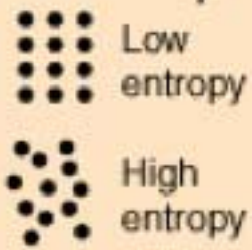

Which came first?

S is more fundamental than E

http://hyperphysics.phy-astr.gsu.edu/hbase/thermo/seclaw.html#c4

Entropy: How to calculate it?

- Test Particle Methods (insertion or deletion)
  - Good for low density systems
  - Perturbation Methods
  - Thermodynamic integration, Thermodynamic perturbation
  - Applicable to most problems
  - Require long simulations to maintain "reversibility"
- Nonequilibrium Methods (Jarzinski's equality)
  - Obtaining differential equilibrium properties from irreversible processes
  - Require multiple samplings to ensure good statistics
- **Normal mode Methods**
  - Good for gas and solids
  - Fast
  - Not applicable for liquids

References: Frenkel, D.; Smit, B. *Understanding Molecular Simulation from Algorithms to Applications*. Academic press: Ed., New York, 2002.
McQuarrie, A. A. *Statistical Mechanics*. Harper & Row: Ed., New York, 1976.
Jarzynski, C. Nonequilibrium Equality for Free Energy Differences. *Phys. Rev. Lett.* 1997, 78, 2690.

If time is not your chief concern….

Solvation free energies of amino acid side chain analogs for common molecular mechanics water models

	Experiment	TIP3P-MOD	TIP3P	SPC	TIP4P	SPC/E	TIP4P-Ew
Ala	1.94	2.18	2.24	2.17	2.25	2.27	2.27
Val	1.99	2.15	2.34	2.41	2.55	2.56	2.63
Ile	2.15	2.10	2.43	2.48	2.68	2.76	2.82
Leu	2.28	2.08	2.27	2.50	2.71	2.75	2.64
Phe	−0.76	−1.31	−0.86	−0.79	−0.65	−0.54	−0.42
Ser	−5.06	−4.58	−4.51	−4.62	−4.71	−4.55	−4.65
Thr	−4.88	−4.42	−4.22	−4.43	−4.47	−4.37	−4.44
Tyr	−6.11	−5.96	−5.46	−5.39	−5.06	−5.07	−4.80
Cys	−1.24	−0.83	−0.55	−0.50	−0.43	−0.33	−0.34
Met	−1.48	−0.78	−0.35	−0.42	−0.07	−0.05	−0.08
Asn	−9.68	−8.88	−8.51	−8.53	−8.52	−8.32	−8.51
Gln	−9.38	−9.02	−8.63	−8.59	−8.49	−8.42	−8.63
Hid	−10.27	−9.36	−8.88	−8.71	−8.66	−8.55	−8.68
Hie	−10.27	−9.46	−9.08	−9.14	−9.10	−8.99	−8.96
Trp	−5.88	−5.55	−4.88	−4.70	−4.14	−4.30	−4.02

Timings: only 8.4 CPU years!

M. R. Shirts and V. S. Pande J. Chem. Phys. **122**, 134508 (2005)

Normal Mode (Harmonic) Analysis

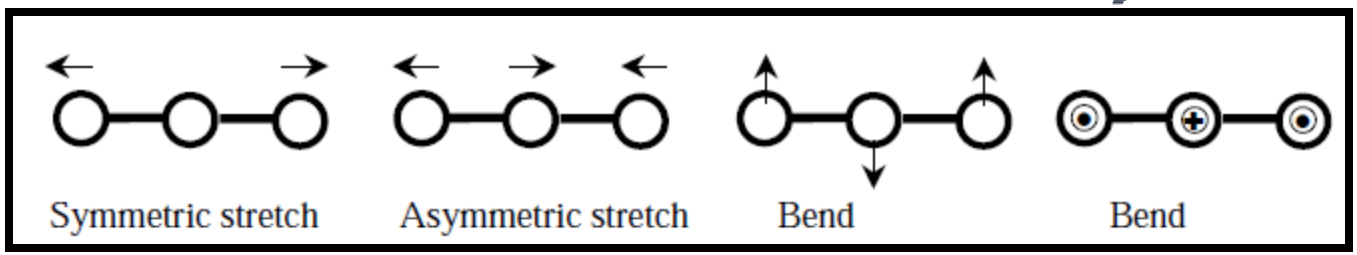

Normal Modes in CO_2

- The density of states *S(υ)*
  - S(υ)dυ number of modes between *υ* and *υ+dυ*

$$\int_0^\infty S(\upsilon)d\upsilon = 3N$$

- Determination of *S(υ)*
  - The eigenvalues of the Hessian matrix (vibrational analysis, phonon spectrum)
  - Covariance matrix of atomic position fluctuations
  - **Fourier transform of velocity autocorrelation function**

$$S(\upsilon) = \frac{2}{kT}\lim_{\tau\to\infty}\int_{-\tau}^{\tau} C(t)e^{-i2\pi\upsilon t}dt \qquad C(t) = \langle v(0)\cdot v(t)\rangle$$

From Normal Modes to Free Energy

- Total number of normal modes = 3N, N=number of particles

- Each vibrational mode can be treated as a harmonic oscillator

$$\varepsilon_n = (n + \frac{1}{2})h\upsilon \qquad q_{HO}^{Q}(\upsilon) = \sum_n \exp(-\beta\varepsilon_n) = \frac{\exp(-\beta h\upsilon/2)}{1 - \exp(-\beta h\upsilon/2)}$$

- The partition function: sum of contributions from HOs

$$\ln Q = \int_0^\infty d\upsilon S(\upsilon) \ln q_{HO}(\upsilon)$$

- All the thermodynamic properties are defined

$$E = V_0 + T\beta^{-1}\left(\frac{\partial \ln Q}{\partial T}\right)_{N,V} \qquad S = k\ln Q + \beta^{-1}\left(\frac{\partial \ln Q}{\partial T}\right)_{N,V}$$

$$A = V_0 - \beta^{-1}\ln Q = V_0 + \beta^{-1}\int_0^\infty d\upsilon S(\upsilon) W_A(\upsilon)$$

Accurate entropies of liquid systems

Fourier Transform VAC to get Density of Vibrational States

Get Enthalpy and Free Energy using quantum partition function

Do 25 picosec MD, Extract Velocity Autocorrelation (VAC) Function

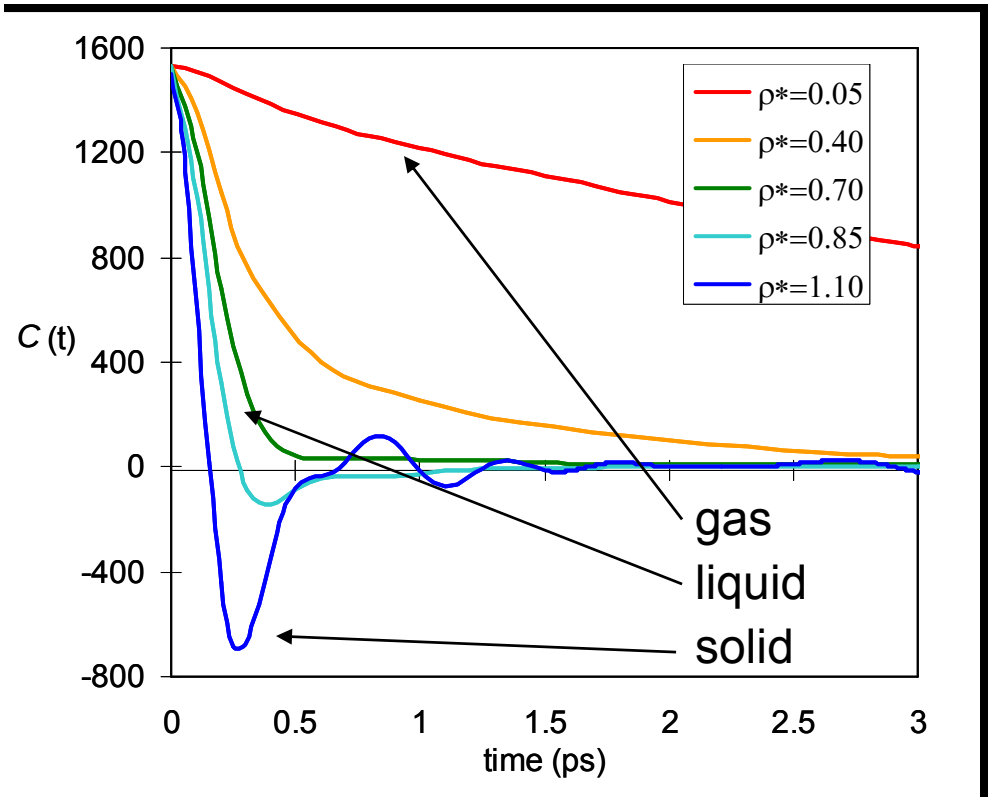

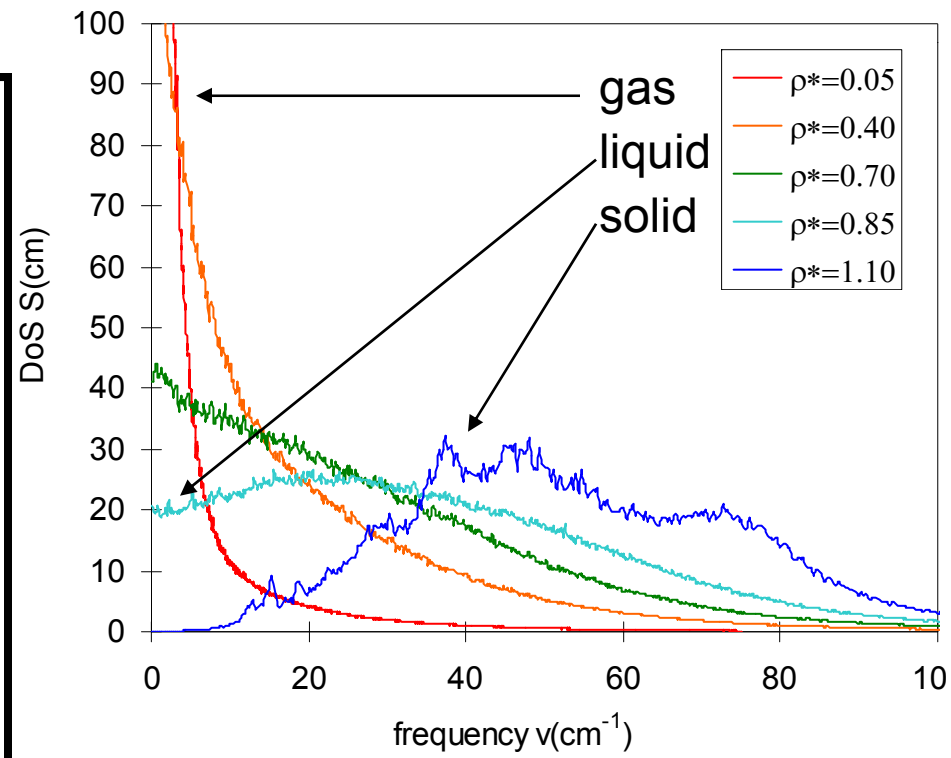

Works well for solids

But there is a problem…

$$q_{HO}^{Q}(\upsilon) = \sum_{n} \exp(-\beta\varepsilon_n) = \frac{\exp(-\beta h\upsilon/2)}{1-\exp(-\beta h\upsilon/2)}$$

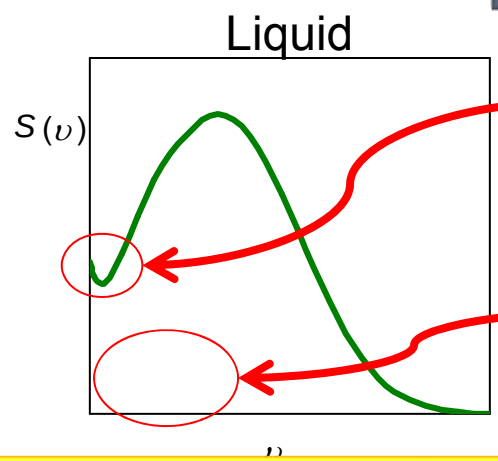

Finite density of states at ν =0

Proportional to diffusion coefficient

Harmonic Approximation → Entropy= ∞

- Also strong anharmonicity at low frequencies

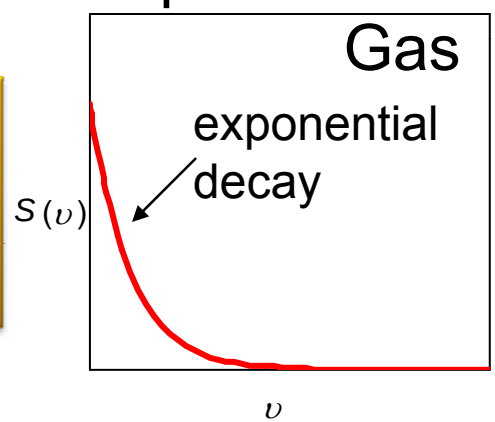

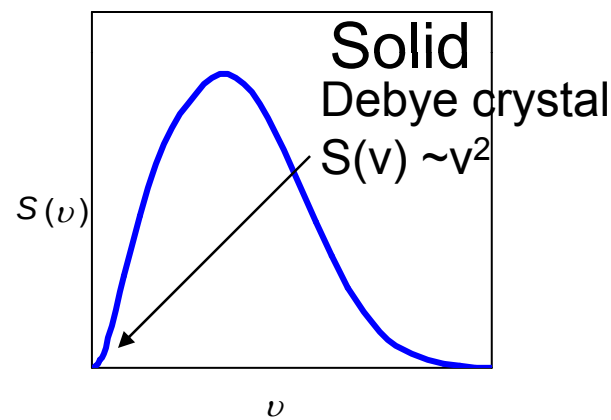

New Model
2 phase theory (2PT)
Liquid ≡ Solid + Gas

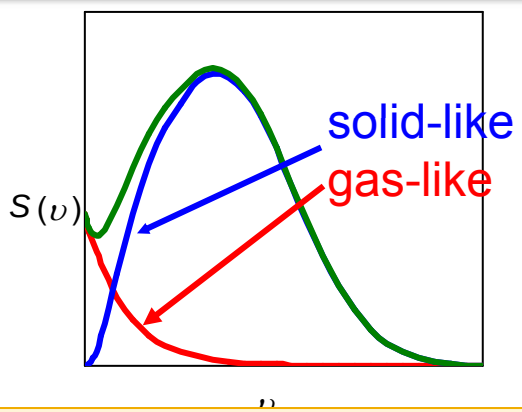

- Two-Phase Thermodynamics Model (2PT)
  - Decompose liquid S(v) to a gas and a solid contribution
  - S(0) attributed to gas phase diffusion
  - Gas component contains anharmonic effects
  - Solid component contains quantum effects

The two-phase model for calculating thermodynamic properties of liquids from molecular dynamics: Validation for the phase diagram of Lennard-Jones fluids; Lin, Blanco, Goddard; JCP, 119:11792(2003)

The 2PT Method

- The basic idea
  - The DoS
  - Thermodynamics
- The gas component
  - VAC for hard sphere gas
  - DoS for hard sphere gas

$$S(\upsilon) = S^{gas}(\upsilon) + S^{solid}(\upsilon)$$

$$P = \int_0^\infty d\upsilon S^g(\upsilon) W_P^g(\upsilon) + \int_0^\infty d\upsilon S^s(\upsilon) W_P^{HO}(\upsilon)$$

$$c^{HS}(t) = \frac{3kT}{m}\exp(-\alpha\, t) \qquad \alpha\,(T, \rho^{HS}, \sigma^{HS}):\ \text{friction coefficient}$$

$$S^{HS}(\upsilon) = \frac{12N^{gas}\alpha}{\alpha^2 + 4\pi^2\upsilon^2} = \frac{s_0}{1 + \left[\dfrac{\pi s_0 \upsilon}{6\, fN}\right]^2}$$

$$N^{gas} = fN$$

$$s_0 = S^{HS}(0) = \frac{12N^{gas}}{\alpha}$$

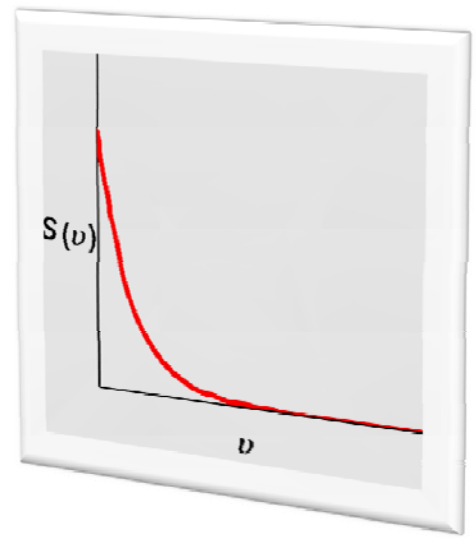

Two unknowns (α and N^{gas}) or (s_o and f)

Determining s_o and f from MD Simulation

- s_o (DoS of the gas component at v=0)
  - completely remove S(0) of the fluid
  - $s_0 = S(0),\ S^{solid}(0) = 0$
- f (gas component fraction)
  - T -> ∞ or ρ -> 0: f -> 1 (all gas)
  - ρ -> ∞: f-> 0 (all solid)

$$f = \frac{D(T,\rho)}{D_0^{HS}(T,\rho;\sigma^{HS})} \qquad D(T,\rho) = \frac{kTs(0)}{12mN}$$

$$D_0^{HS}(T,\rho;\sigma^{HS}) = \frac{3}{8}\frac{1}{\rho\sigma^{HS\,2}}\left(\frac{kT}{\pi m}\right)^{1/2} \quad \text{(Chapman - Enskog)}$$

one unknown σ^{HS}

Determining σ^{HS}

- σ^{HS} (hard sphere radius for describing the gas molecules)
- gas component diffusivity should agree with statistical mechanical predictions at the same T and ρ
- gas component diffusivity from MD simulation

$$D^{HS}(T, f\rho) = \frac{kTs_0}{12mfN}$$

- HS diffusivity from the Enskog theory

$$D^{HS}(T, f\rho) = D_0^{HS}(T, f\rho; \sigma^{HS}) \frac{4fy}{z(fy) - 1}$$

$y = \frac{\pi}{6}\rho\sigma^{HS\,3}$ Hard sphere packing fraction

$z(y) = \frac{1 + y + y^2 - y^3}{(1-y)^3}$ Compressibility

And finally….

- A universal equation for *f*

$$2\Delta^{-9/2} f^{15/2} - 6\Delta^{-3} f^{5} - \Delta^{-3/2} y^{7/2} + 6\Delta^{-3/2} f^{5/2} + 2f - 2 = 0$$

$$\text{normalized diffusivity}: \ \Delta(T,\rho,m,s_0) = \frac{2s_0}{9N}\left(\frac{\pi kT}{m}\right)^{1/2} \rho^{1/3} \left(\frac{6}{\pi}\right)^{2/3}$$

- Graphical representation

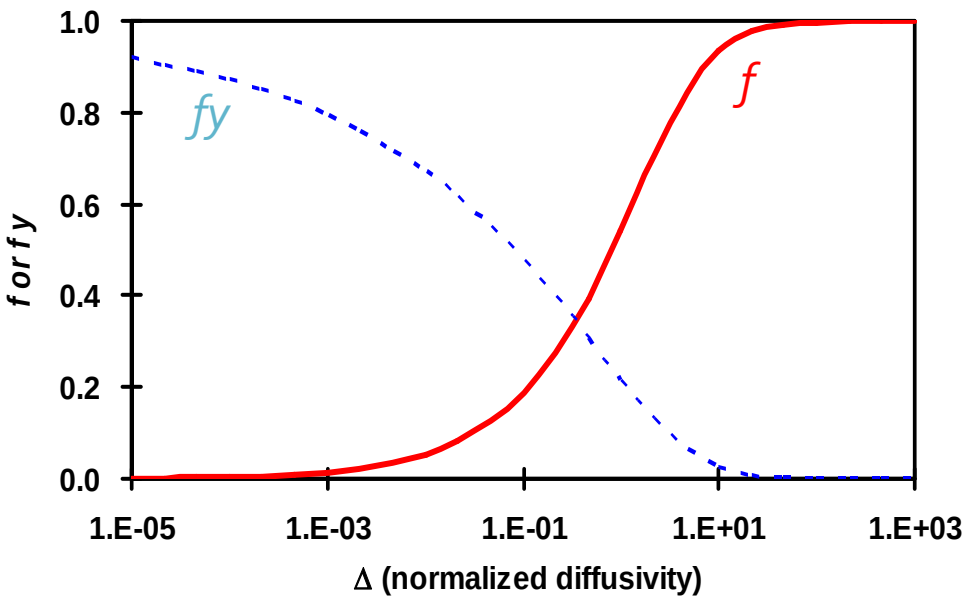

Computational Scheme

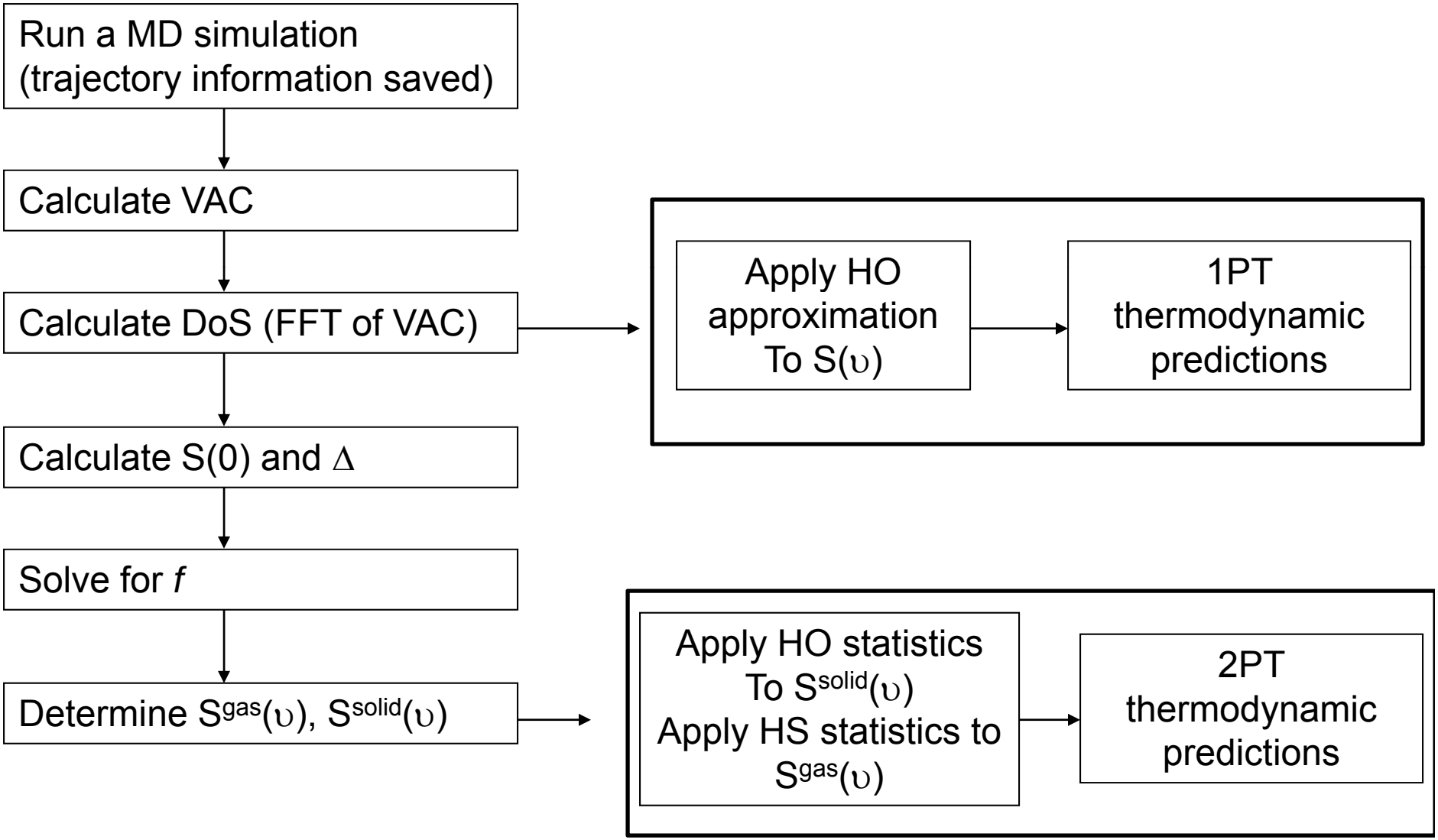

Test case 1: Lennard Jones Fluid

- Intermolecular potential

$$V(r) = 4\varepsilon\left[\left(\frac{\sigma}{r}\right)^{12} - \left(\frac{\sigma}{r}\right)^{6}\right]$$

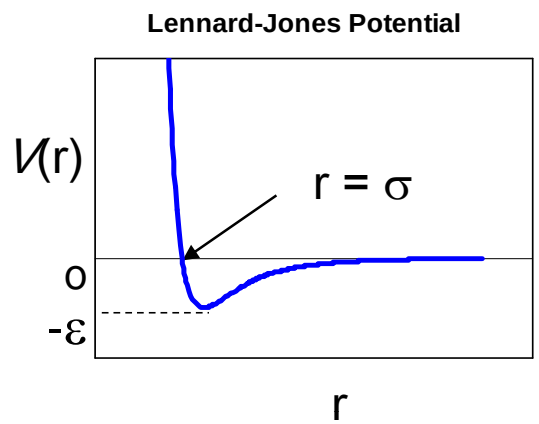

- Phase diagram
  - critical point

$$T_c^* = 1.316 \pm 0.006$$

$$\rho_c^* = 0.304 \pm 0.006$$

  - triple point

$$T_{tp}^* \approx 0.69$$

($T^*=kT/\varepsilon$ $\rho^*=\rho\sigma^3$)

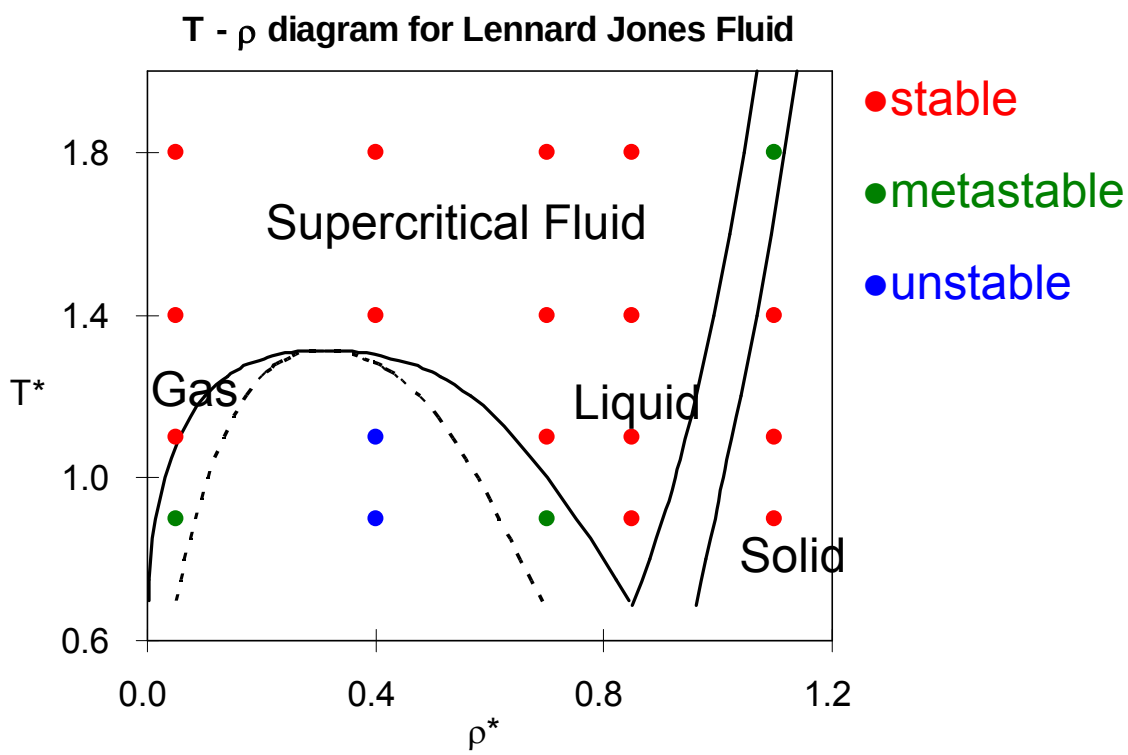

LJ VAC and DoS

Velocity Autocorrelation

$$C(t) = \langle v(0) \cdot v(t) \rangle$$

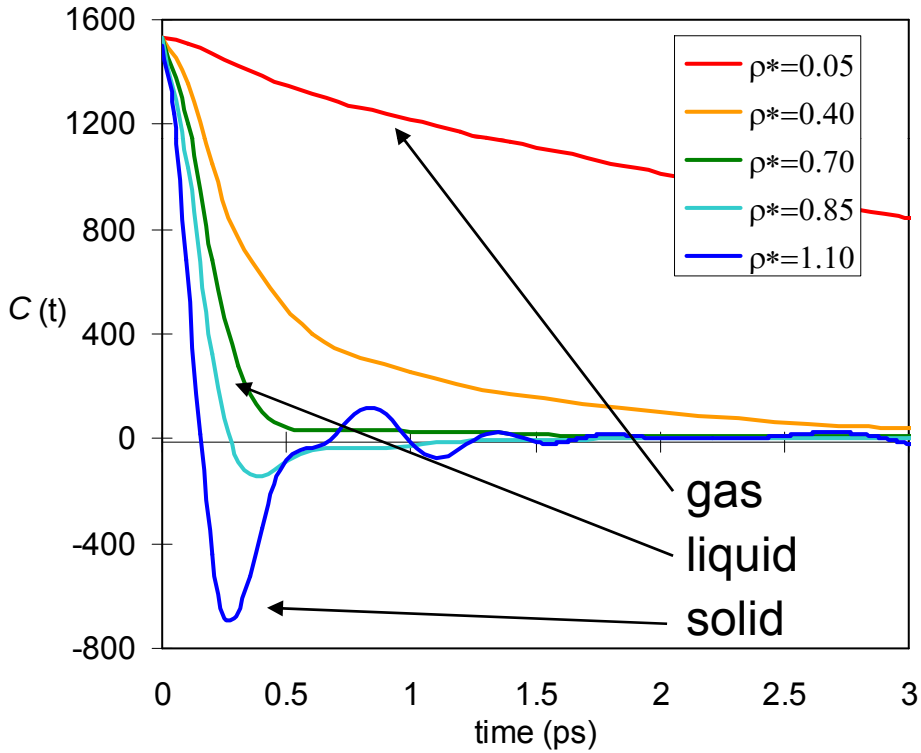

Density of States

$$S(\upsilon) = \frac{2}{kT} \lim_{\tau - \infty} \int_{-\tau}^{\tau} C(t) e^{-i2\pi\upsilon t} dt$$

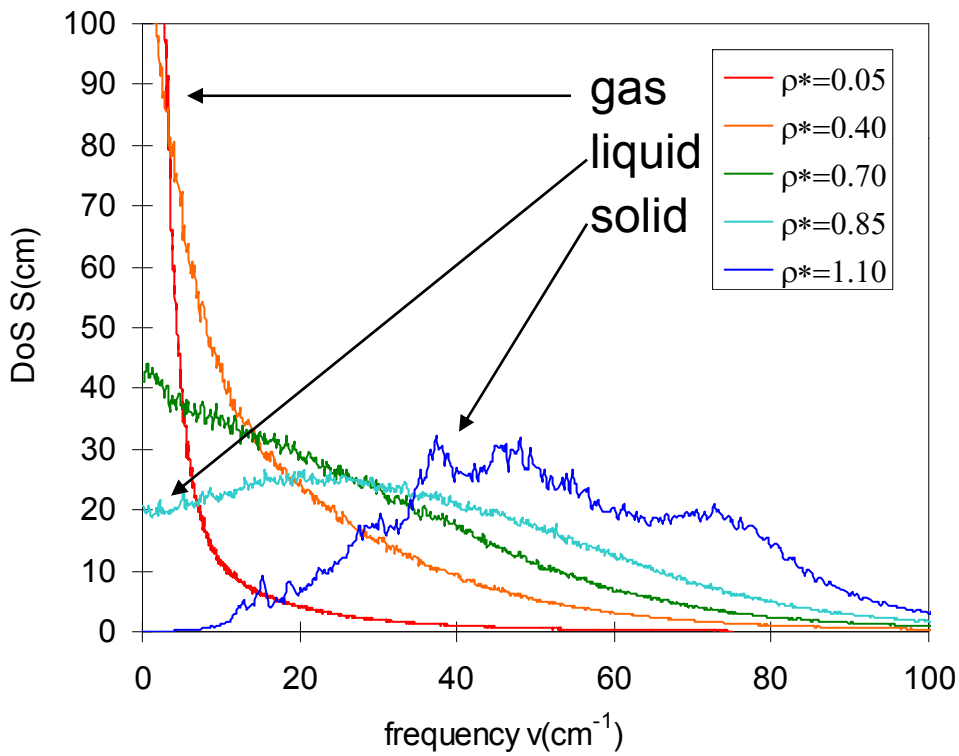

2PT DoS Decomposition

- Examples

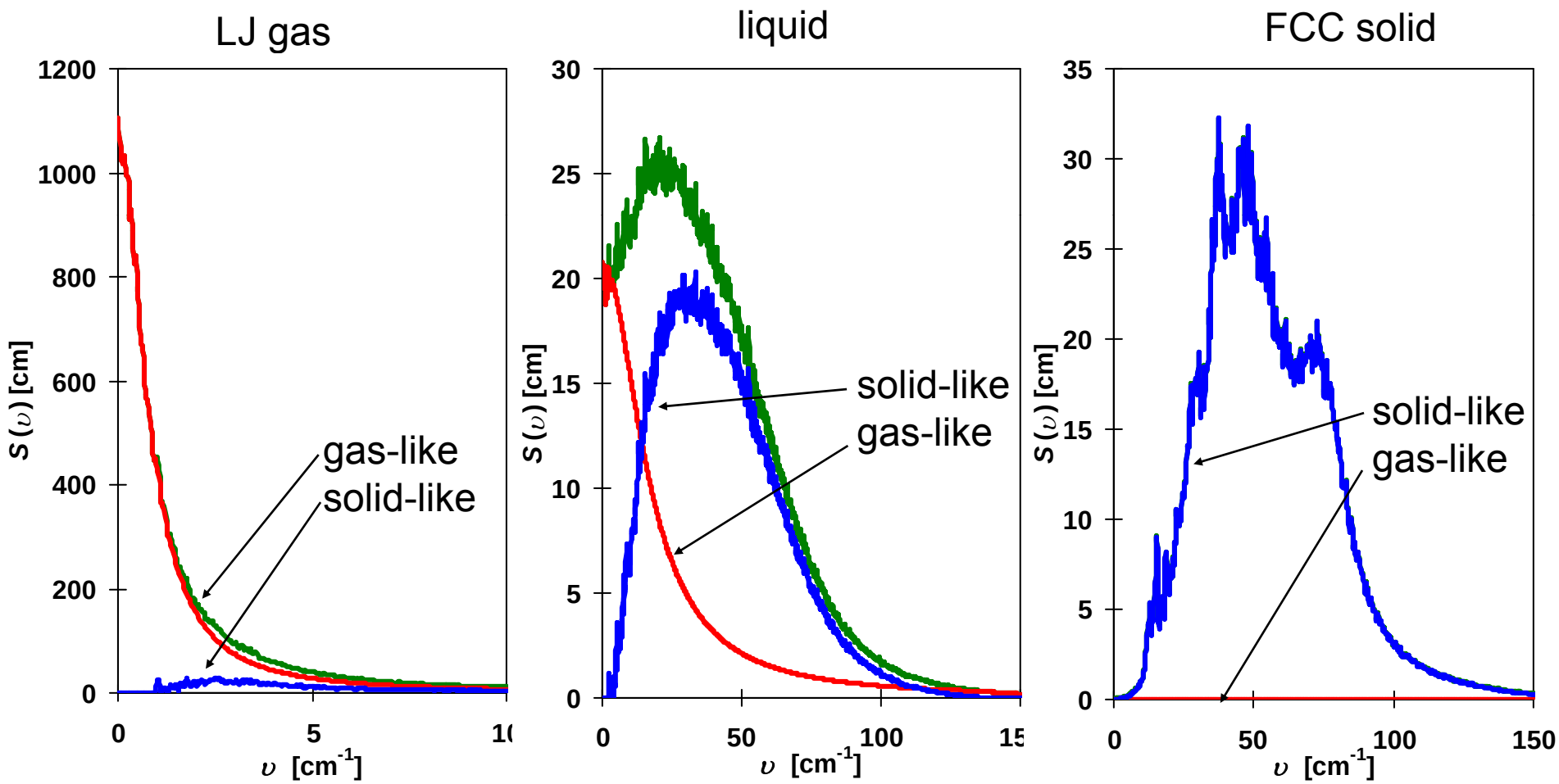

Pressure and Energy for LJ Gas

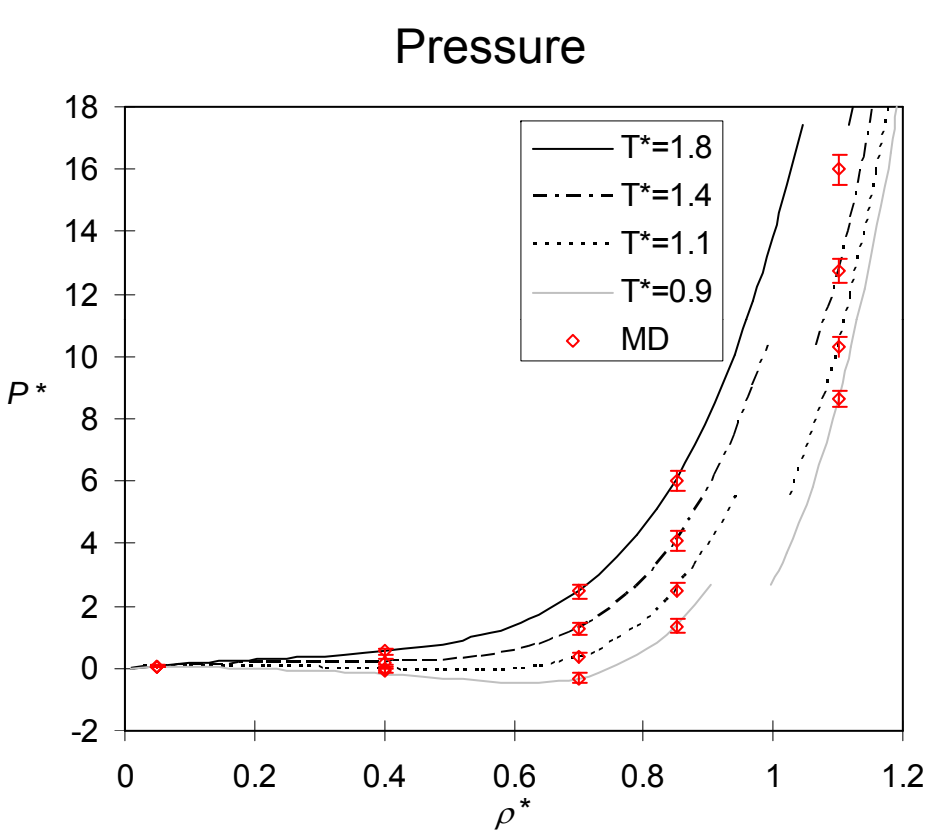

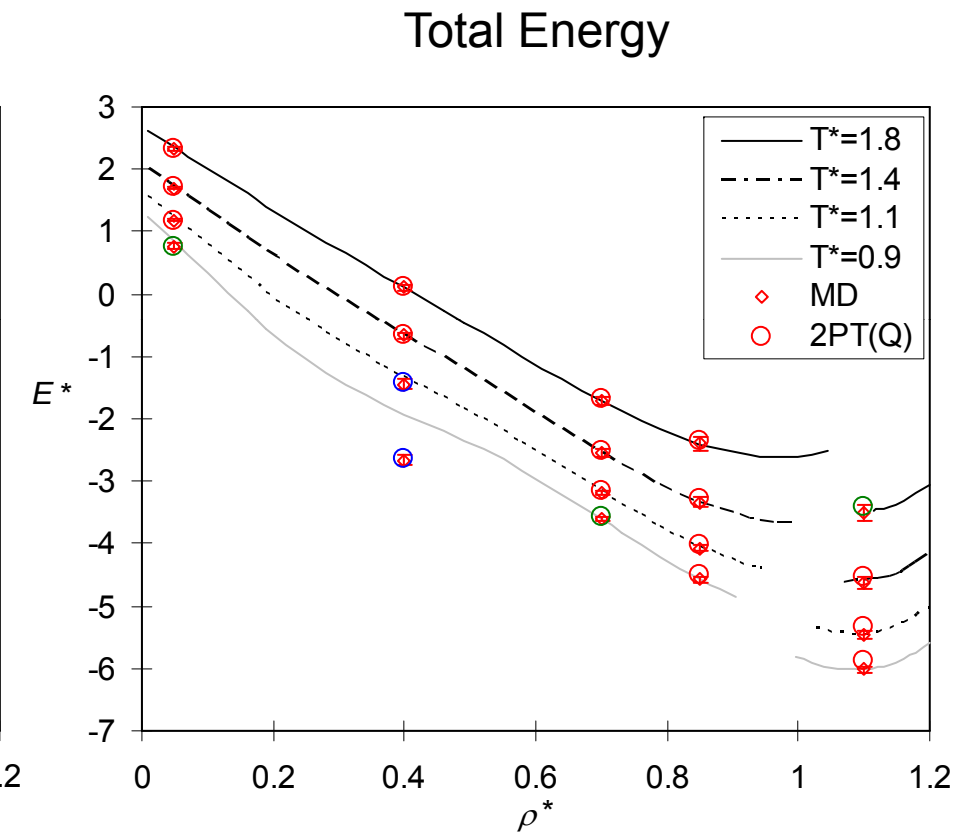

Pressures and MD Energies agree with EOS values
Quantum Effect (ZPE) most significant for crystals (~2%)

Entropy

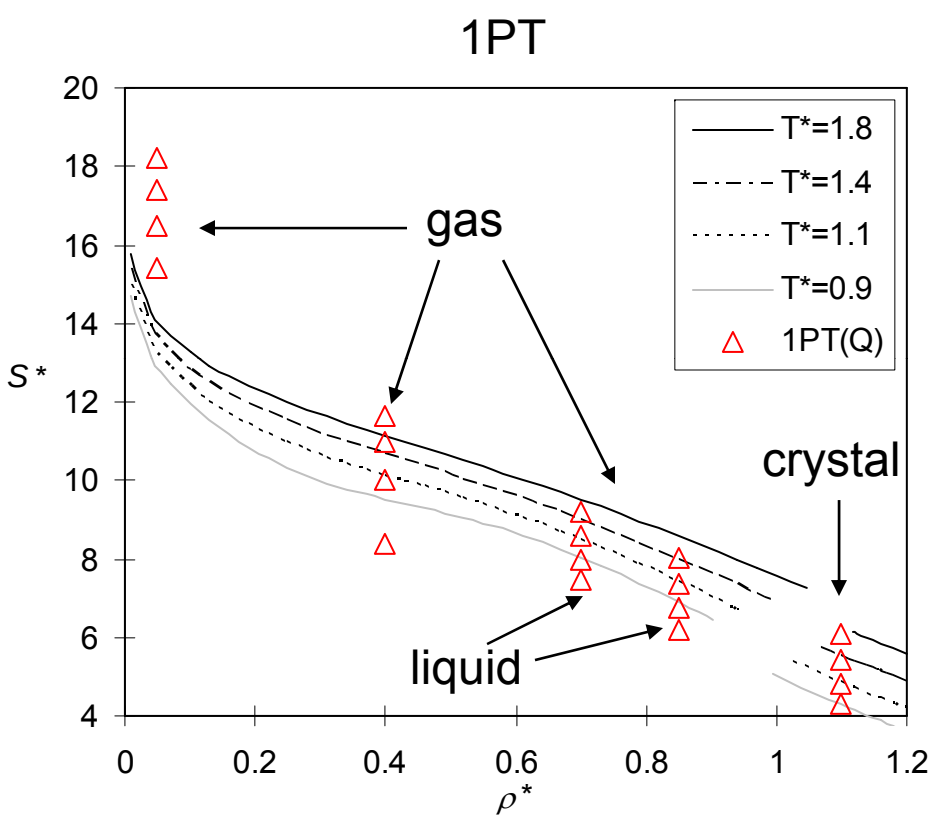

- Overestimate entropy for low density gases
- Underestimate entropy for liquids
- Accurate for crystals

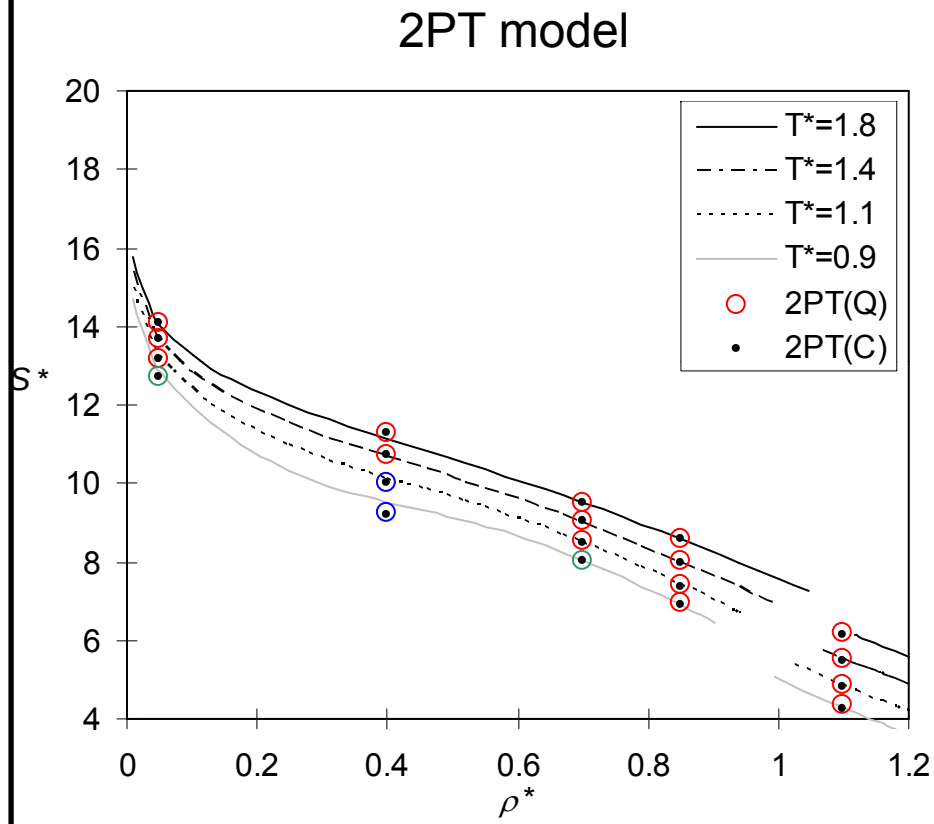

- Accurate for gas, liquid, and crystal
- Accurate in metastable regime
- Quantum Effects most important for crystals (~1.5%)

Gibbs Free Energy

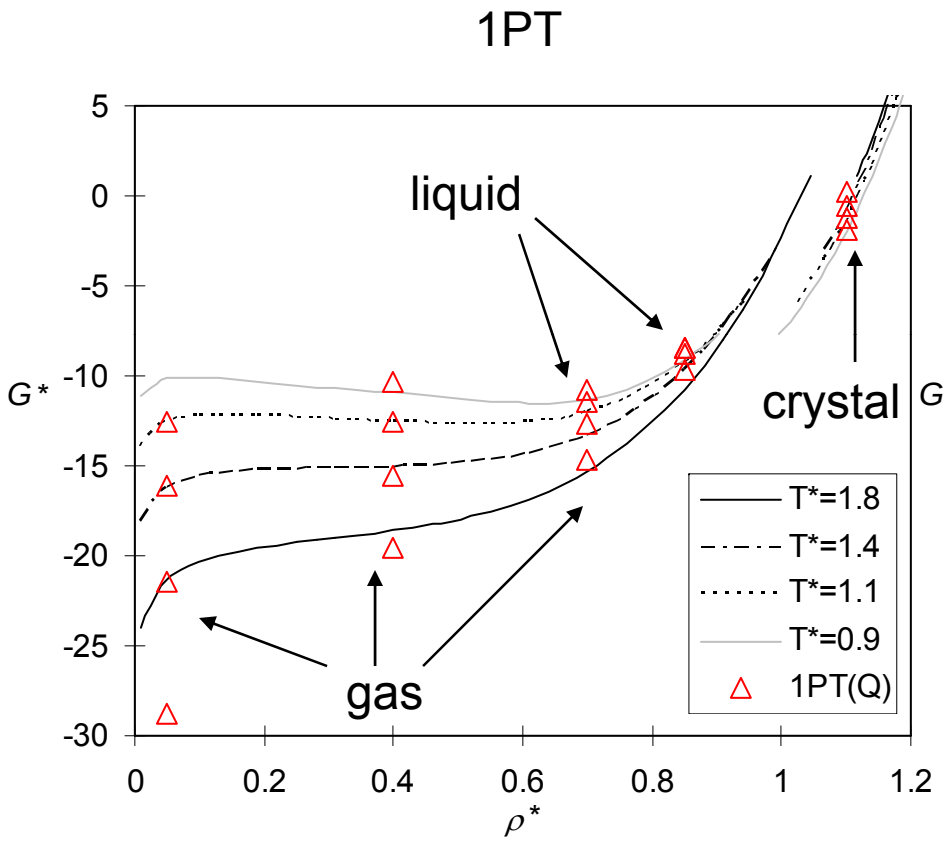

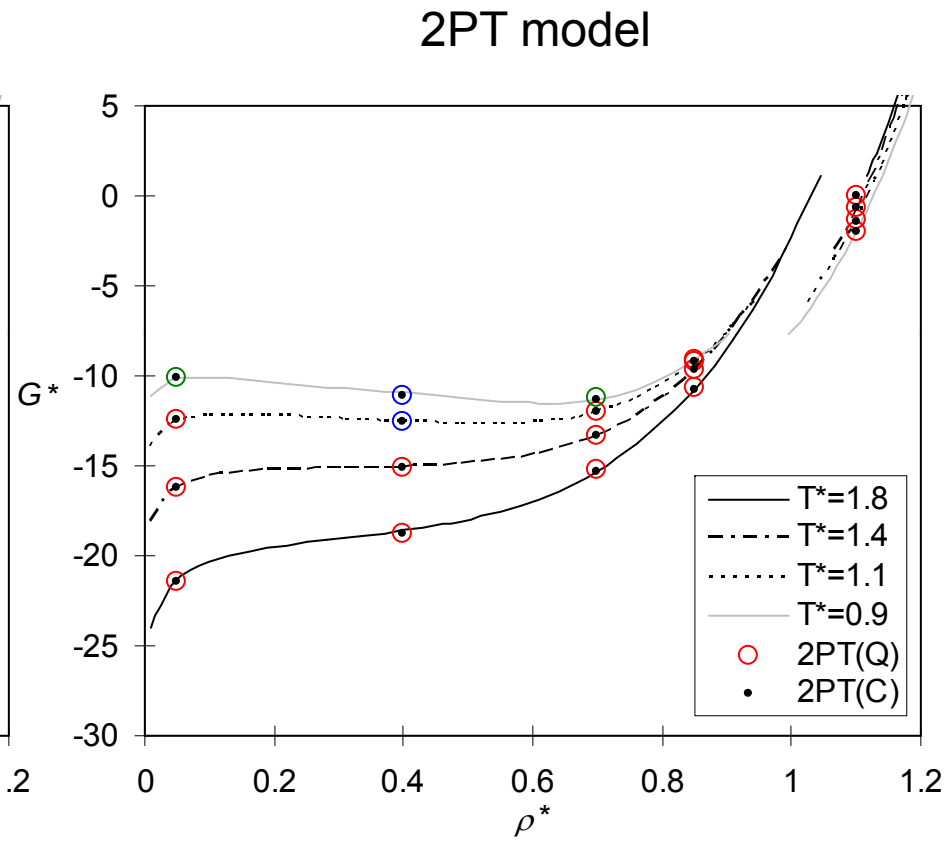

- Underestimate free energy for low density gases
- overestimate entropy for liquids
- Accurate for crystals

- Accurate for gas, liquid, and crystal
- Accurate in metastable regime

Why does 2PT work?

$$P = \int_0^\infty d\upsilon S^s(\upsilon) W_P^{HO}(\upsilon) + \int_0^\infty d\upsilon S^g(\upsilon) W_P^g(\upsilon)$$

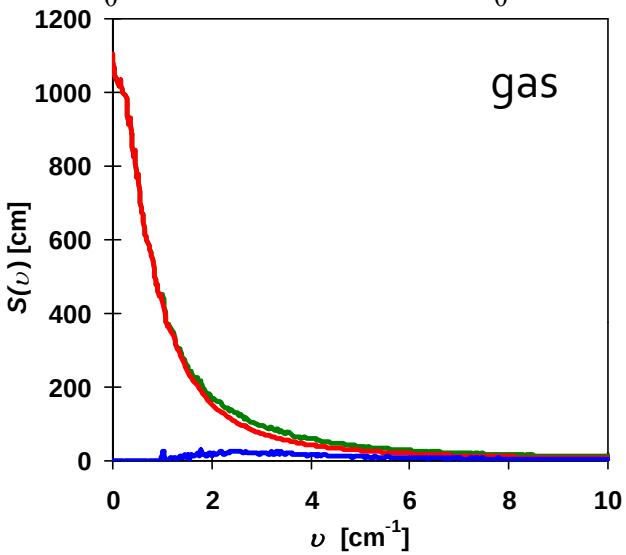

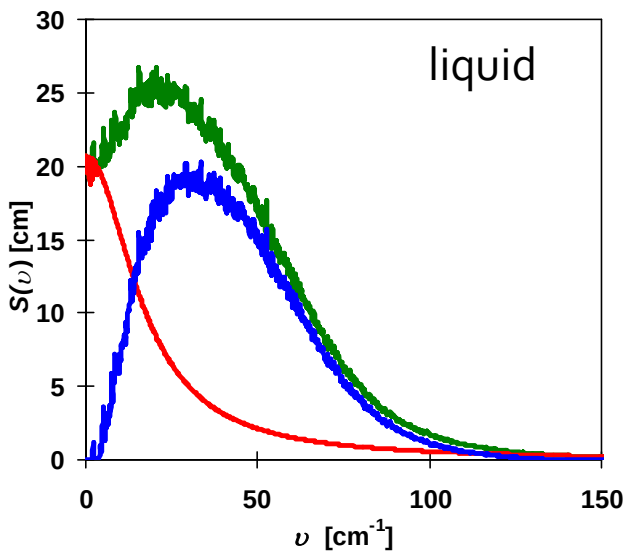

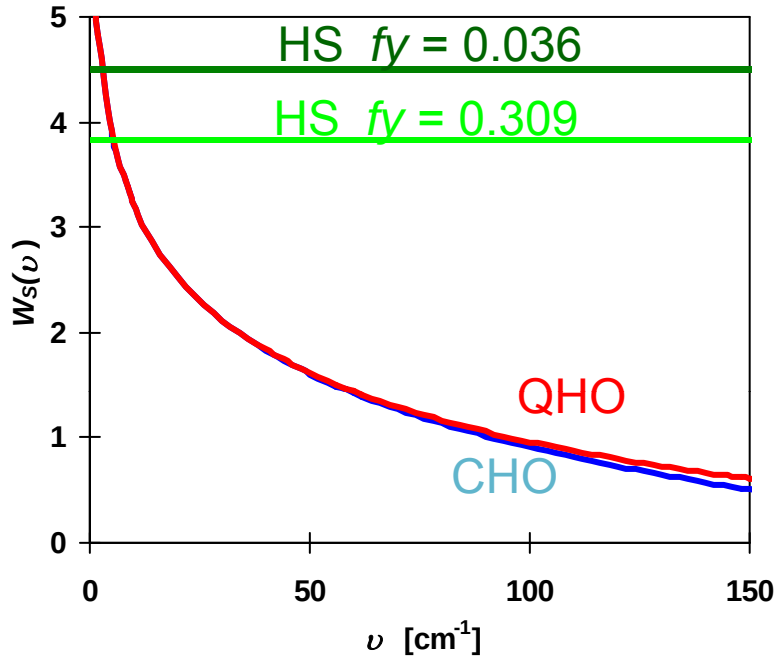

- 1PT overestimates W_s^{gas} for gas for modes < 5 cm^{-1}
- 1PT underestimates W_s^{gas} for liquid for modes between 5 and 100 cm^{-1}
- 2PT properly corrects these errors

Convergence of 2PT

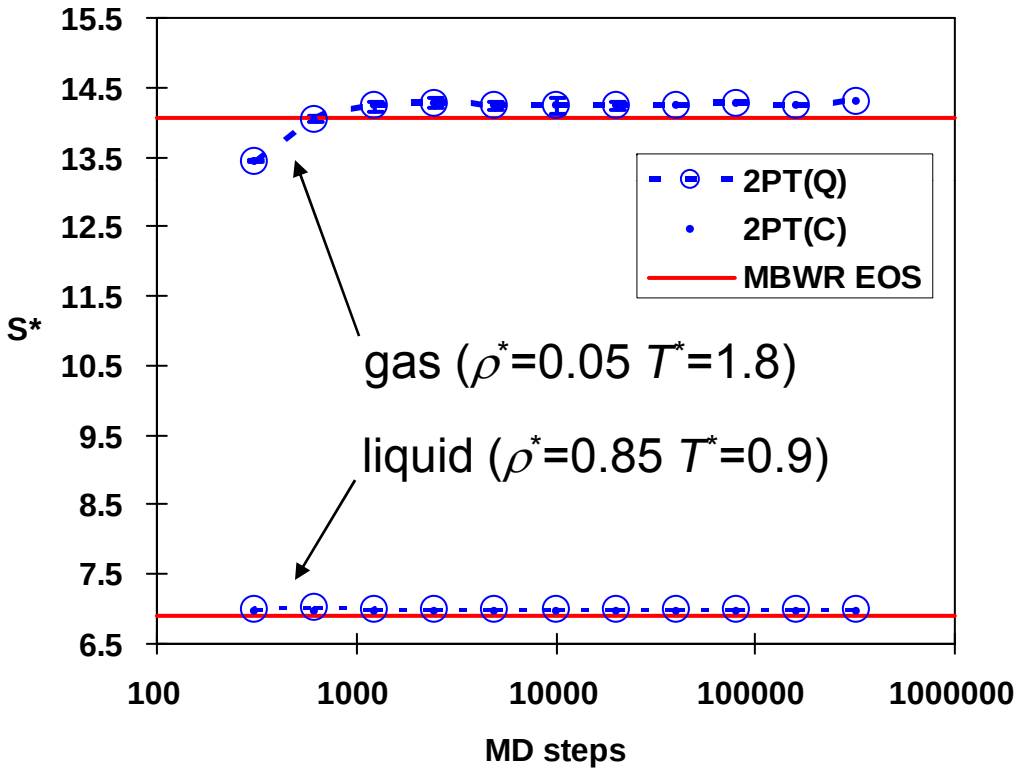

- For gas, the entropy converges to within 0.2% with 2500 MD steps (20 ps)
- For liquid, the entropy converges to within 1.5% with 2500 MD steps (20 ps).

Melting and Solidification

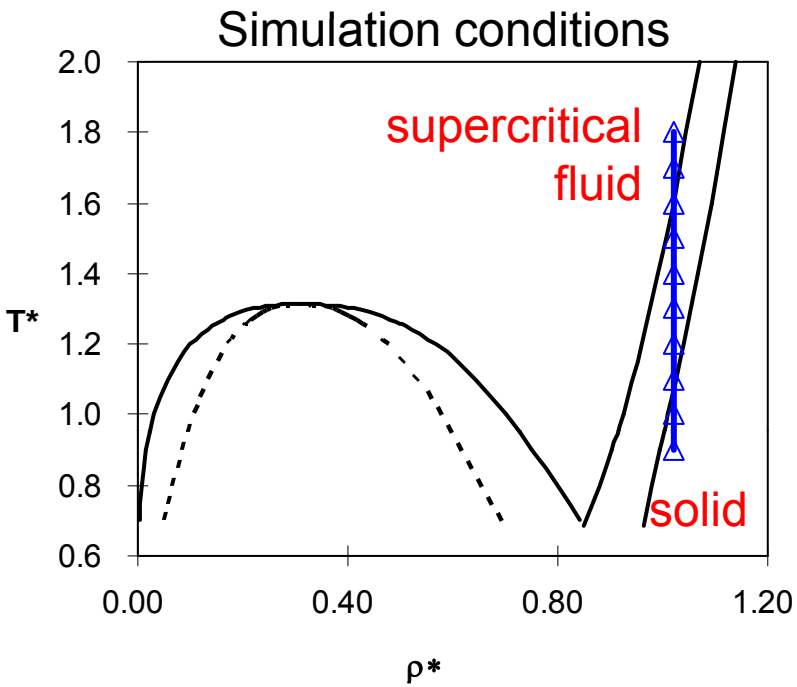

- Initial amorphous structure is used in the cooling process
- The fluid remains amorphous in simulation even down to T*=0.8 (supercooled)
- The predicted entropy for the fluid and supercooled fluid agree well with EOS for LJ fluids

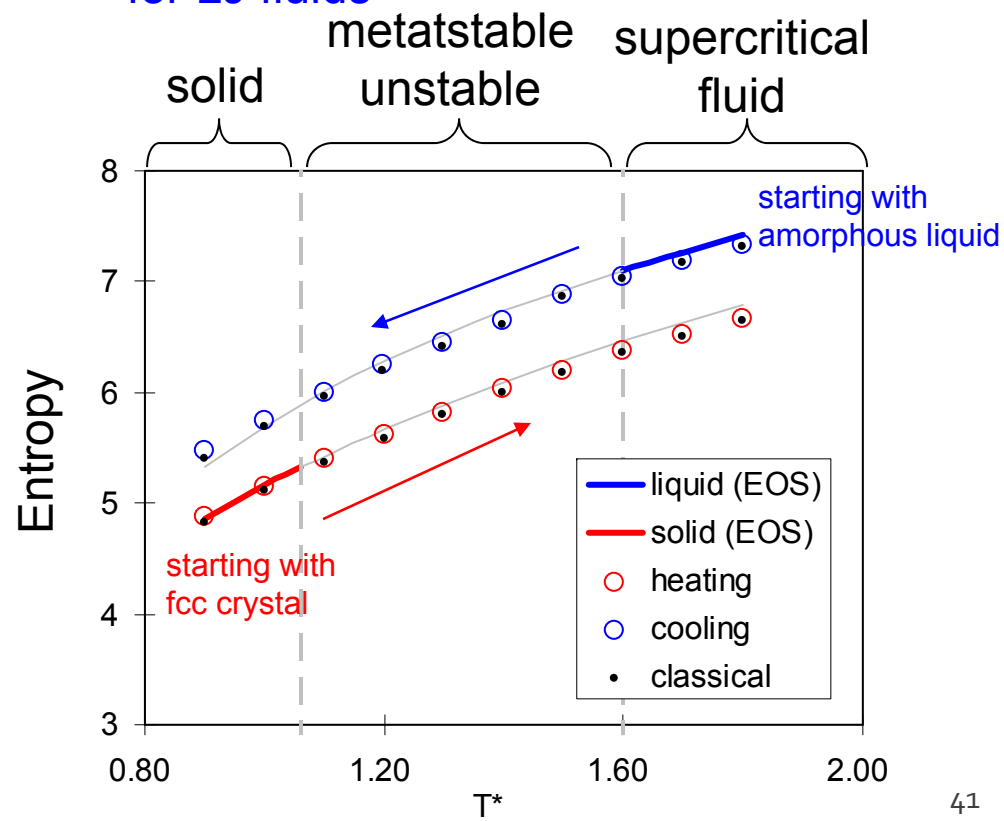

- Initial fcc crystal is used in the heating process
- The crystal appears stable in simulation even up to T*=1.8 (superheated)
- The predicted entropies for the crystal and superheated crystal agree well with EOS for LJ solids

Water Power Spectrum (DoS) (25 ps, 1fs steps)

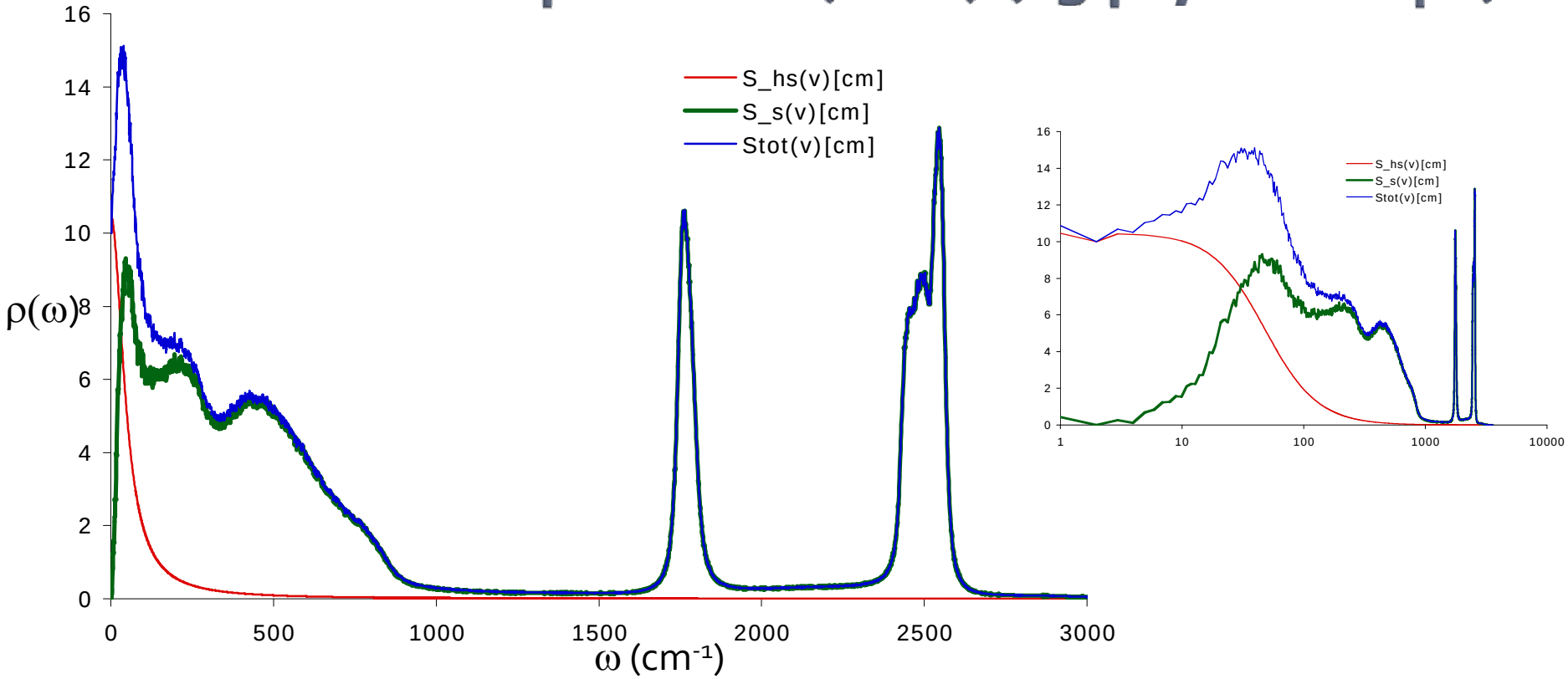

Power spectrum for water at 300 K. The power spectrum is decomposed into a gas (diffusive) and a solid (fixed) spectra and their contributions added to yield the free energy of the liquid state.

Power spectrum for water at 300 K. The power spectrum is decomposed into a gas (diffusive) and a solid (fixed) spectra and their contributions added to yield the free energy of the liquid state.

Entropy of water box

Iteration	s_solid	s_liquid	s_total	sq/molecule	Volume	Density
1	26306.42	29263.86	55570.29	69.46285763	24504.28	0.975681
2	29171.87	26448.94	55620.8	69.52600088	23907.47	1.000037
3	28149.65	27416.01	55565.66	69.45707063	24350.23	0.981853
4	27695.09	28090.08	55785.18	69.73146913	24708.74	0.967607
5	28518.58	27110.11	55628.69	69.53585838	24546.61	0.973998
6	27281.02	28656.05	55937.07	69.92133425	24536.97	0.974381
7	25557.95	29920.17	55478.12	69.347647	24771.36	0.965161
8	28725.58	27031.59	55757.17	69.69646113	24393.49	0.980112
9	28970.64	26858.49	55829.14	69.786419	24647.06	0.970028
10	27409.63	28214.45	55624.08	69.53010463	24353.55	0.981719
Average	27778.64	27900.98	55679.62	69.59952226	24471.98	0.977058
Std Dev	1175.371	1127.951	141.6069	0.177008662	245.1435	0.009893

- Theory: 69.6 +/- 0.2 J/K*mol
- Experimental Entropy: 69.9 J/K*mol (NIST)

Statistics collected over 20ps of dynamics , no additional computation cost

The Harmonic Osicllator

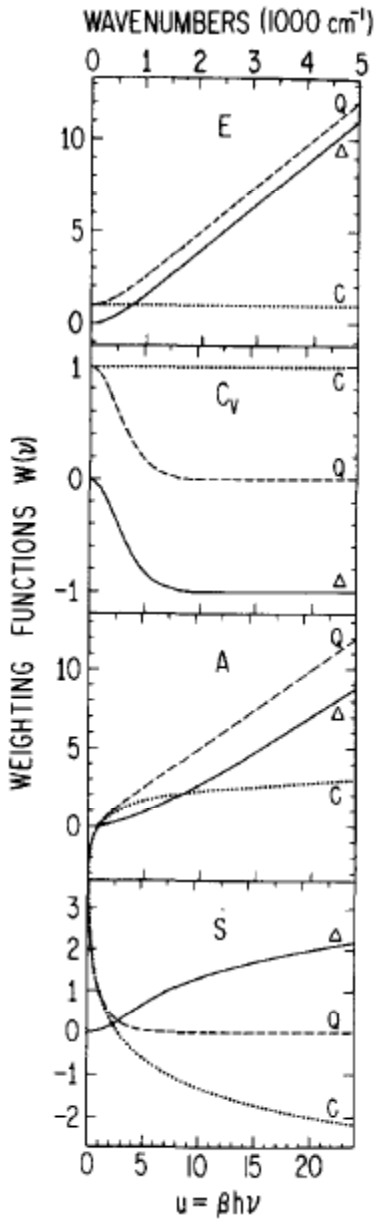

- HO weighting functions
  - Classical $q^C(\nu) = (\beta h\nu)^{-1} = u^{-1}$

$$E^C = V_0 + k_B T \int_0^\infty d\nu\, S(\nu) W_E^C(\nu) \; ; \quad W_E^C(\nu) = 1 \, ,$$

$$C_v^C = k_B \int_0^\infty d\nu\, S(\nu) W_{C_v}^C(\nu) \; ; \quad W_{C_v}^C(\nu) = 1 \, ,$$

$$A^C = V_0 + k_B T \int_0^\infty d\nu\, S(\nu) W_A^C(\nu) \; ; \quad W_A^C(\nu) = \ln u$$

$$S^C = k_B \int_0^\infty d\nu\, S(\nu) W_S^C(\nu) \; ; \quad W_S^C(\nu) = [1 - \ln u] \, .$$

  - Quantum $q^Q(\nu) = \dfrac{e^{-u/2}}{1 - e^{-u}}$

$$E^Q = V_0 + k_B T \int_0^\infty d\nu\, S(\nu)\, W_E^Q(\nu) \; ; \quad W_E^Q(\nu) = \left(\frac{u}{2} + \frac{u}{e^u - 1}\right)$$

$$C_v^Q = k_B \int_0^\infty d\nu\, S(\nu) W_{C_v}^Q(\nu) \; ; \quad W_{C_v}^Q(\nu) = \left(\frac{u^2 e^u}{(1 - e^u)^2}\right)$$

$$A^Q = V_0 + k_B T \int_0^\infty d\nu\, S(\nu) W_A^Q(\nu) \; ; \quad W_A^Q(\nu) = \left(\ln \frac{1 - e^{-u}}{e^{-u/2}}\right)$$

$$S^Q = k_B \int_0^\infty d\nu\, S(\nu) W_S^Q(\nu) \; ; \quad W_S^Q(\nu) = \left(\frac{u}{e^u - 1} - \ln(1 - e^{-u})\right)$$

Quantum effects in Molecular systems

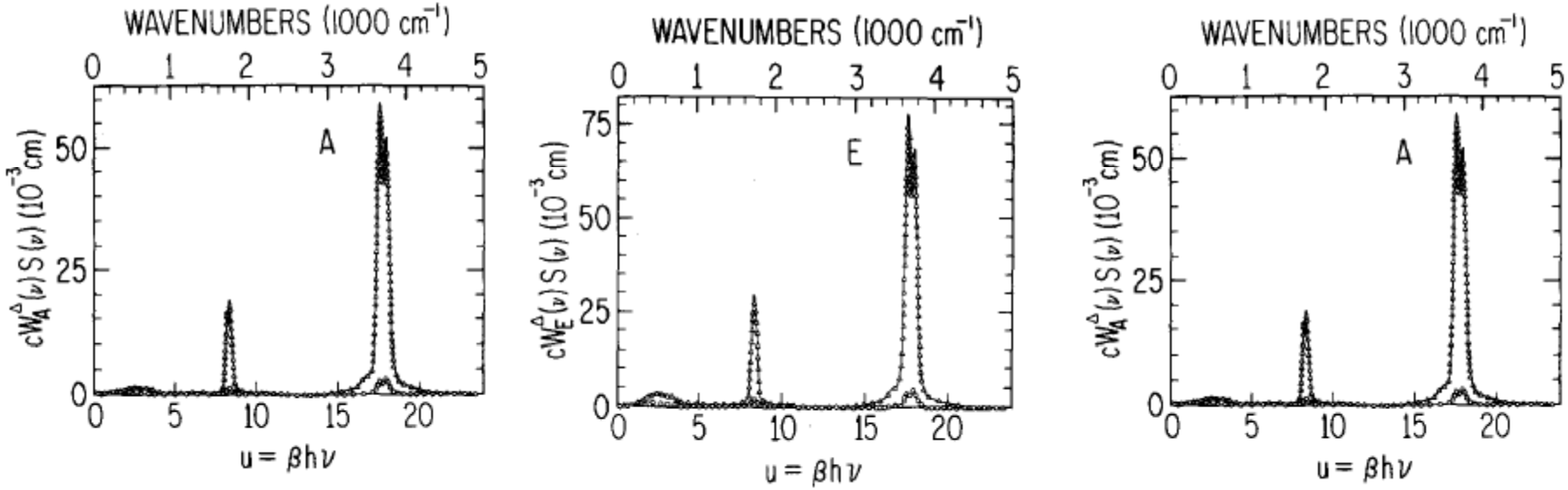

TABLE I. Inter- and intramolecular contributions to liquid water quantum corrections at 300 K per mole.

	Inter (0–1200 cm^{-1})	Intra (1200–5000 cm^{-1})	Total
E^{Δ} (kJ)	4.2	45.0	49.2
C_v^{Δ} (J/K)	−11.0	−23.8	−34.8
A^{Δ} (kJ)	2.2	33.4	35.6
S^{Δ} (J/K)	6.5	38.8	45.3

- Quantum effects largest in high frequency modes
- Quantum Entropy correction is positive
  - Quantum harmonic oscillator $h\nu >> k_bT$: stuck in ground state
  - Classical harmonic oscillators has contribution from infinite number of states

Co2 Phase Diagram

Physical Properties

Molar mass	44.010 g/mol
Appearance	colorless, odorless gas
Density	1.562 g/mL (solid/1 atm/195K) 0.770 g/mL (liquid/56 atm293K) 1.977 g/L (gas /1 atm/273K) 849.6 g/L (supercritical/150 atm/305K)
Melting point	194.7 K
Boiling point	216.6 K (at 5.185 bar)
Solubility in water	1.45 g/L at 300K/1 bar
Acidity (pKa)	6.35, 10.33
Viscosity	0.07 cP/195K
Dipole moment	0

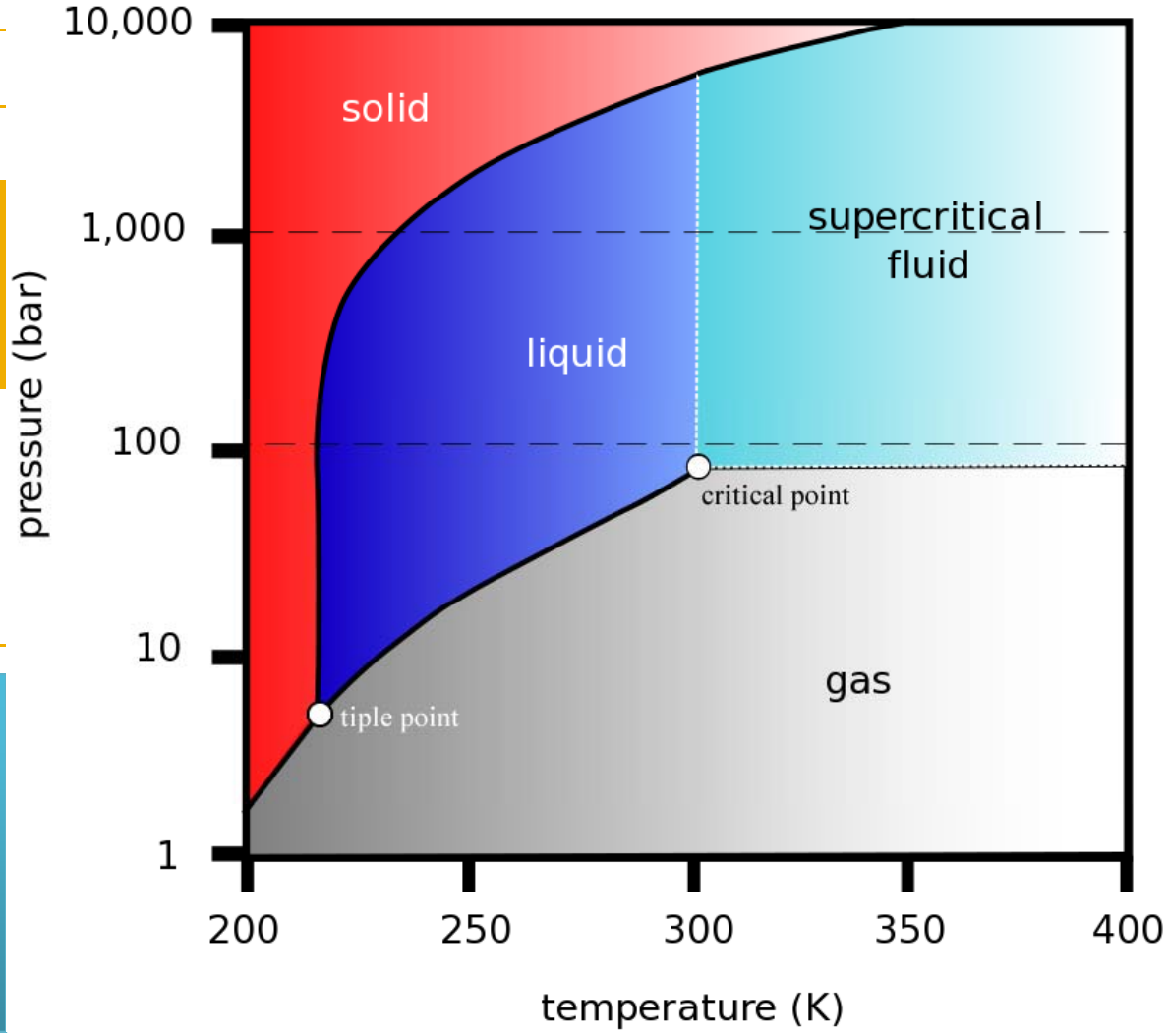

Issues with current approaches

- CPMD simulations (32 molecules) too small to describe phase behavior
- Rigid empirical models give inaccurate super-critical behavior
- Flexible empirical model not fit to thermodynamic properties

Needs accurate forcefields that accounts for physical and thermodynamic properties

Empirical forcefields for Co2

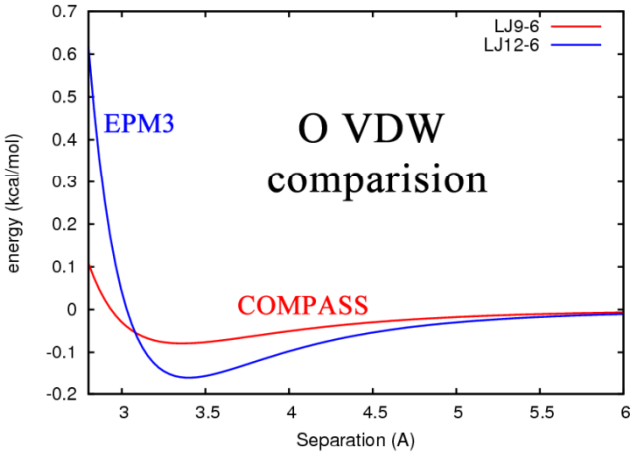

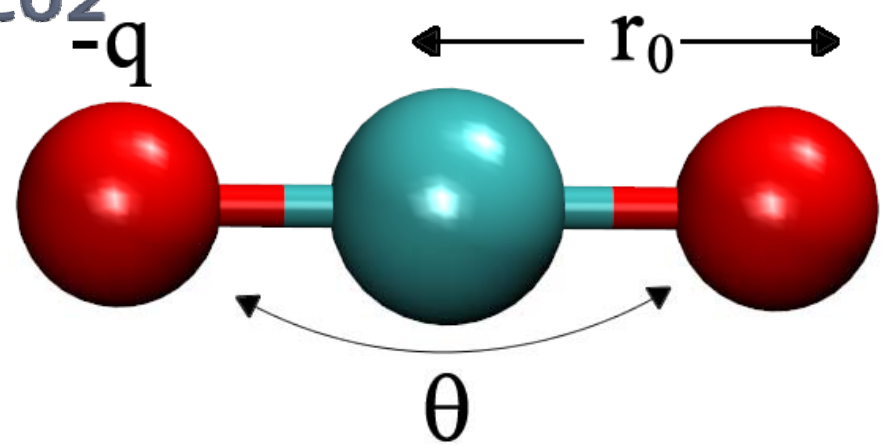

	ε_C	σ_C	ε_O	σ_O	α	q_C	r_o
[1]MSM	0.058	2.785	0.165	3.01	-	0.596	1.160
[2]EPM2	0.056	2.757	0.160	3.03	-	0.651	1.149
[3]EPM3	0.056	2.800	0.160	3.03	-	0.652	1.162
[4]TraPPE	0.054	2.800	0.157	3.05	-	0.700	1.160
[5]Errington*	0.058	2.753	0.165	3.03	14	0.647	1.143
[6]Zhang	0.057	2.792	0.164	3.00	-	0.589	1.163
[7]COMPASS*	0.136	3.420	0.134	2.94	-	0.800	1.160

Critical Properties

	T_c(K)	ρ_c (g/cm³)	P_c (MPa)
	304.9	0.4642	7.17
	303.2	0.4664	7.07
	304.0	0.4679	7.39
	309.1	0.462	7.2
	302.5	0.4728	7.31
	304.0	0.467	7.23
	316.1	0.4621	6.92
Exp	304.1	0.4676	7.377

- Errington uses Exponential-6 for VDW
- COMPASS uses Bond-Bond stretch term to match vib. frequencies
- Models optimized to reproduce experimental physical properties

How well do they reproduce experimental thermodynamics?

EoS over phase diagram

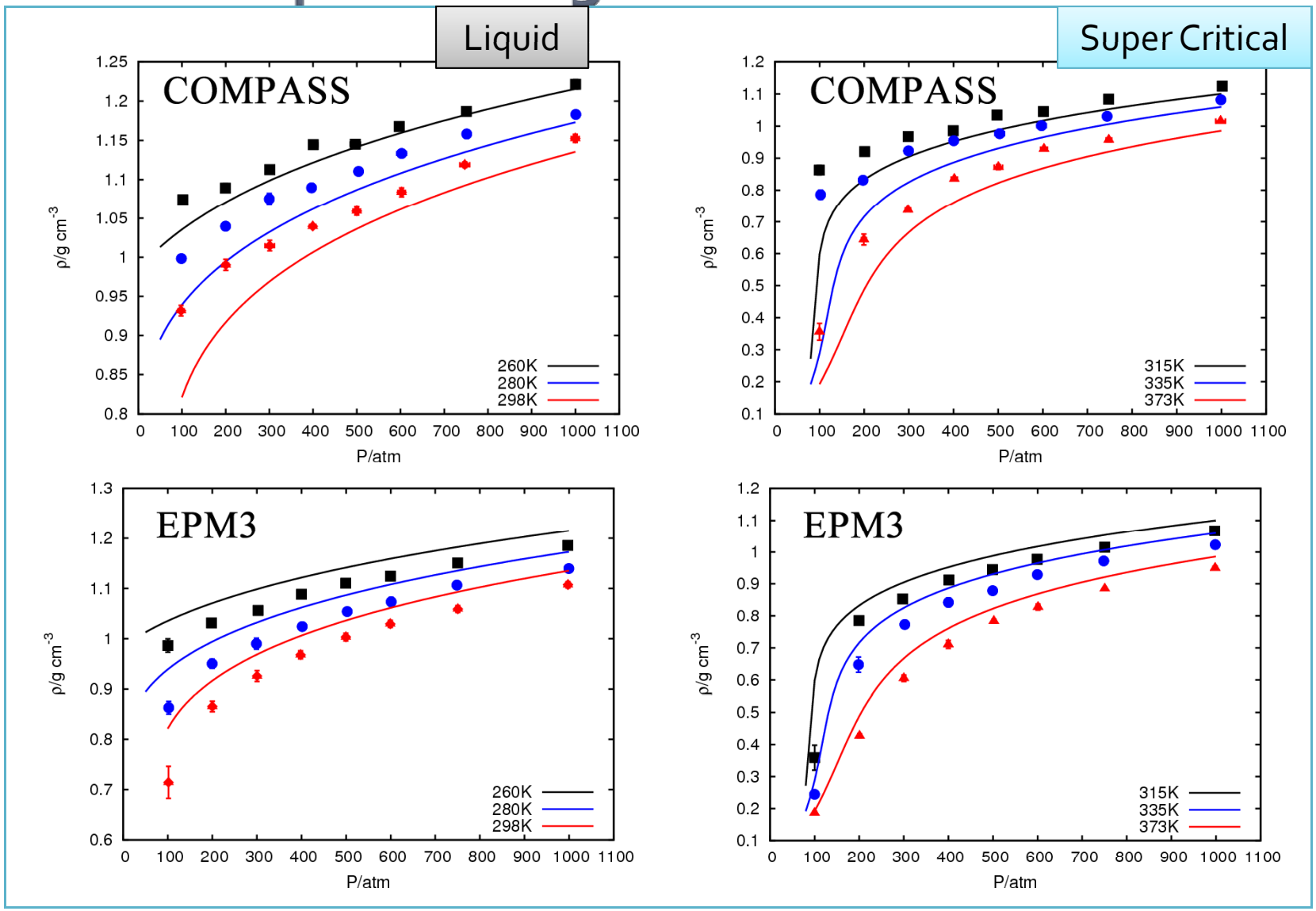

- COMPASS has reasonable description of liquid, poor description of Sc-Co2 at low pressures
- EPM3 more accurate for both liquid and Sc-Co2

Standard Molar entropy over phase diagram

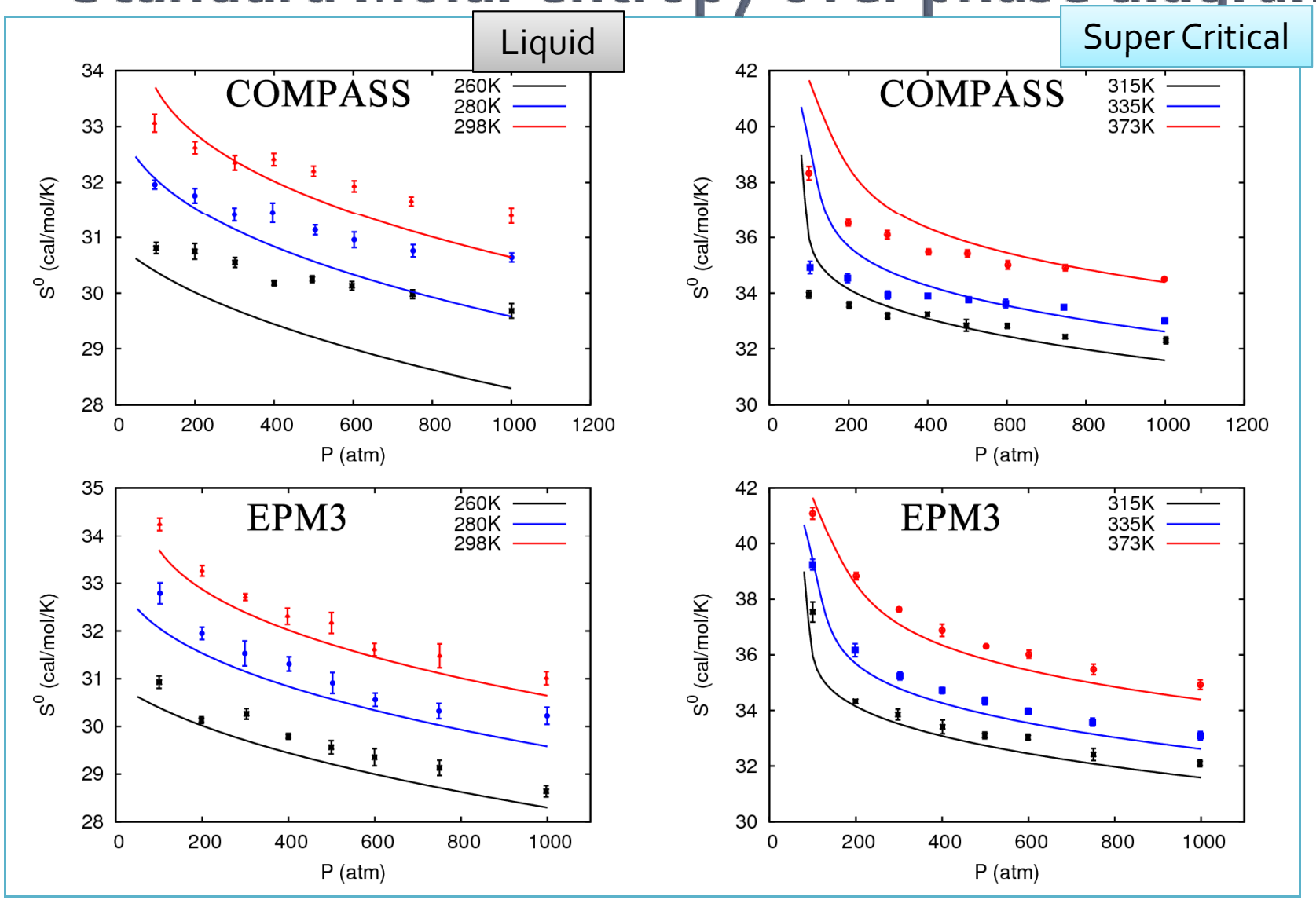

- COMPASS has large errors at high pressure liquid phase
- EPM3 superior for both liquid and Sc-CO_2

Melting of dry ice

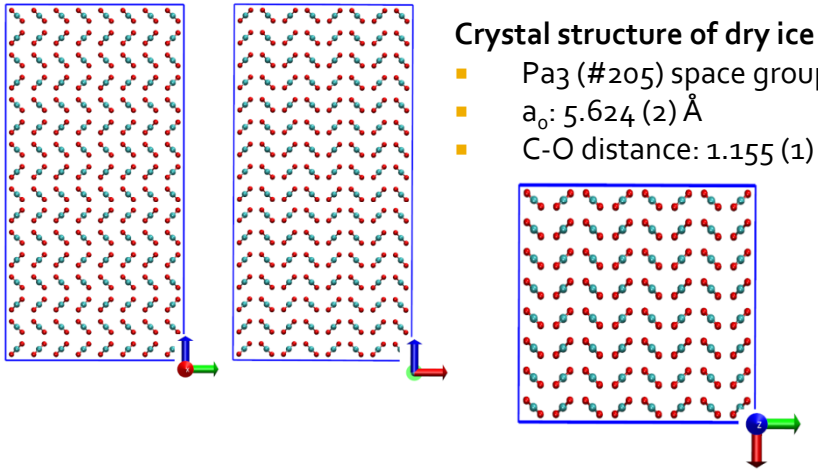

Crystal structure of dry ice

- Pa3 (#205) space group
- a_o: 5.624 (2) Å
- C-O distance: 1.155 (1) Å

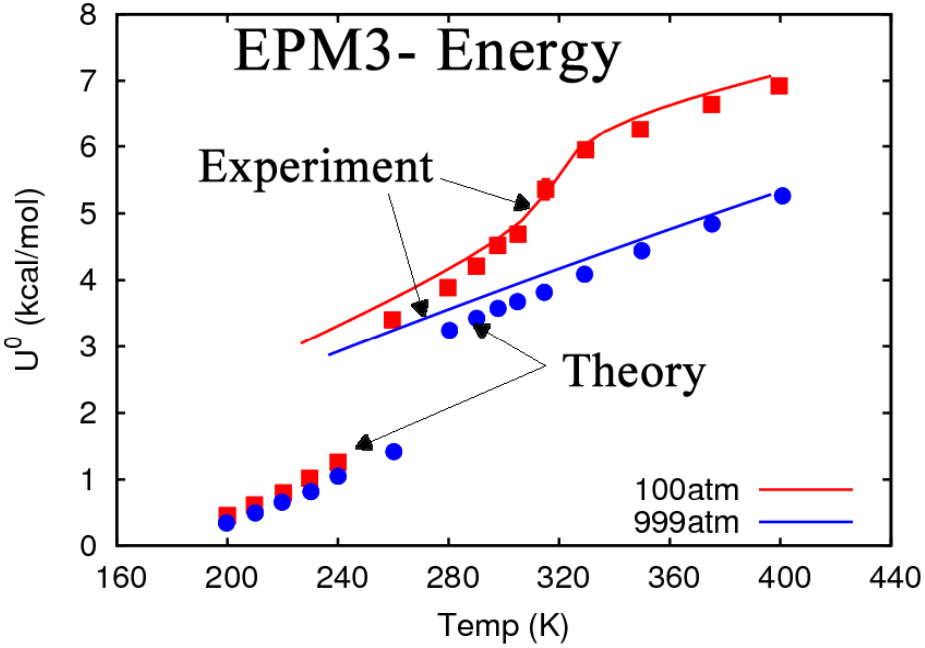

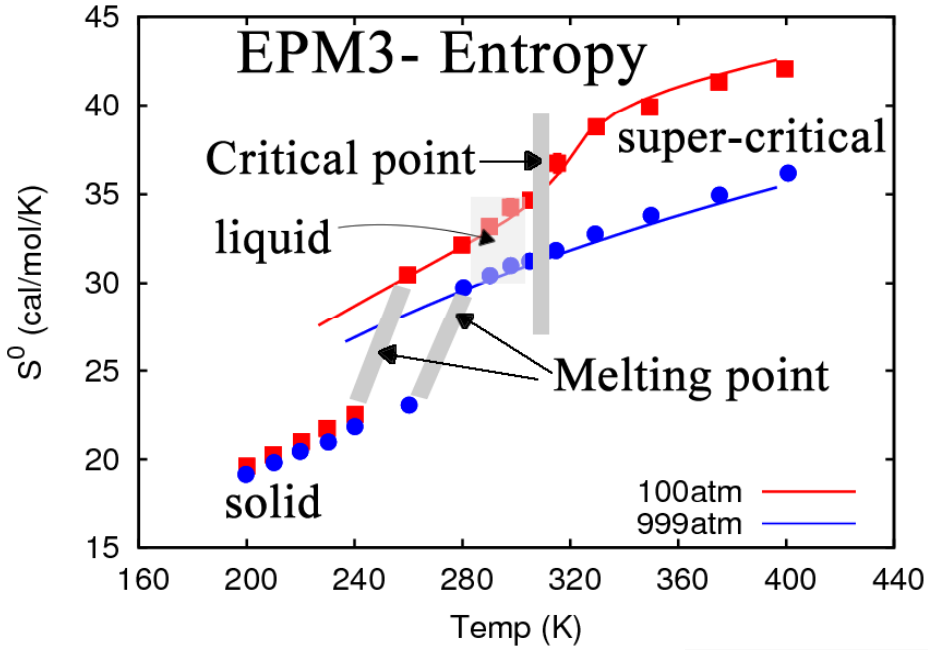

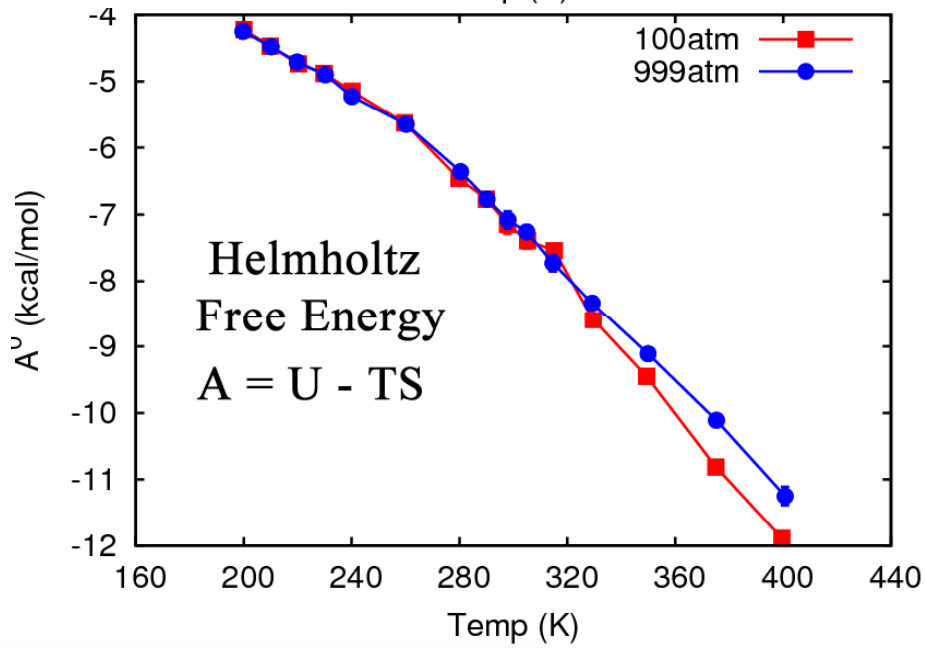

Free Energy is dominated by entropy

Components of entropy

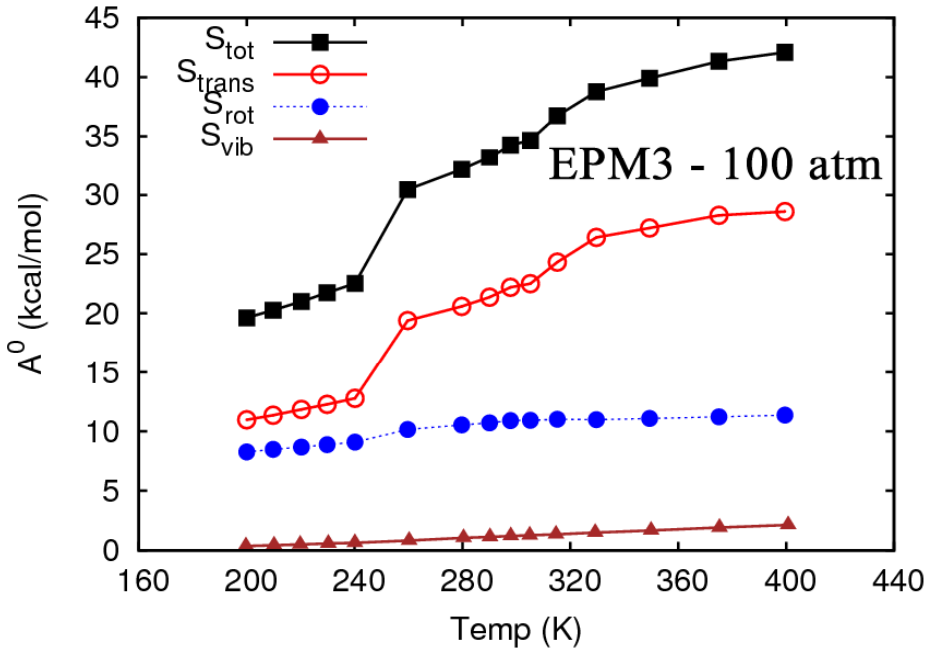

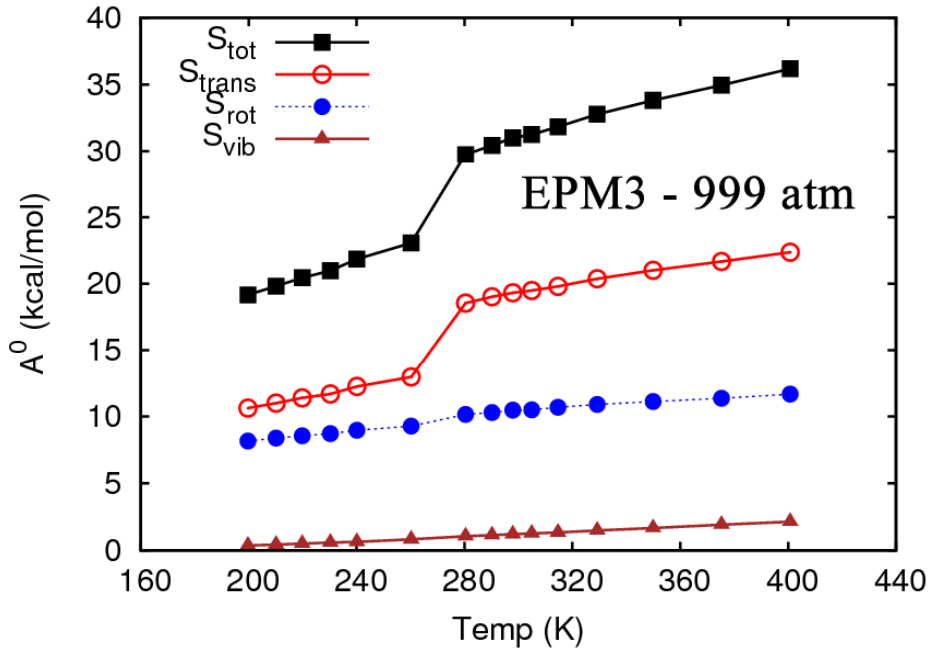

- Entropy dominated by diffusion (50 % - solid, 55% liquid, 66% super critical
- Melting of Co2 corresponding to dramatic increase in diffusional entropy
- Small increase in rotational entropy: Co2 not a free rotor in liquid phase
- Monotonic increase in vibrational entropy from solid-> liquid ->super critical

Conculsion

- The recent EMP3 forcefield is accurate at describing the physical and thermodynamics of liquid and Sc-Co2
  - Correctly predicts critical properties
  - Melting temperature is 20K too high
- COMPASS forcefield is not as accurate
- Free Energy is dominated by entropy
- Diffusional entropy accounts for 50 – 66% of total entropy

Project Schedule

- MONTH 1-12 --- Identification of the Mid-IR spectra of DIC species under normal conditions through DFT QM simulations, verified by existing data and preliminary FTIR data.
- MONTH 13-24 --- Simulation and obtain preliminary FTIR MIR spectra of DIC species under changed conditions, i.e. high temperature and pressure, through ReaxFF simulations
- MONTH 25-36 --- Simulation of the MIR spectra changes under the underground brine water conditions and chemistry.

MILESTONE LOG

- MONTH 1-12 --- Identification of the Mid-IR spectra of DIC species under normal conditions through DFT QM simulations, verified by existing data and preliminary FTIR data.
- MONTH 13-24 --- Simulation and obtain preliminary FTIR MIR spectra of DIC species under changed conditions, i.e. high temperature and pressure, through ReaxFF simulations
- MONTH 25-36 --- Simulation of the MIR spectra changes under the underground brine water conditions and chemistry.

perceived risks in the proposed technical research

- QM simulations provide information at 0K and zero pressure
- The ReaxFF simulation parameters must be tuned and calibrated against rigorous QM calculations for 0K and zero pressure
- For high temperature and pressure QM cannot provide the needed data. Here we must rely on ReaxFF with validations from experiment.
- The intensities for HCO_3- spectra are not known experimentlally. They might be weak compared to dissolved CO_2 and could be buried in the strong water absorption bands. This might make Mid-IR measurement of HCO3- impractical.

We will use the following approaches to identify, analyze and respond to the perceived risks associated with the proposed project.

We will use ReaxFF to provide an alternative or a further improvement to classic QM DFT simulation to account for high temperature and pressure; although this process takes back and forth tuning, MSC has the expertise to conduct such tuning
TO provide a calibration for ReaxFF simulation under high temperature and pressure, we will conduct limited FTIR measurement of very thin lasers of samples under high temperature and pressures and provide a proof of principle experimental results for REAX tuning.
If HCO_3^- does not have an optimal band in the Mid-IR for detection, we will concentrate on CO_2 dissolved measurement and spectra, because it is already demonstrated that under high temperature and pressure, brine water already have pretty low pH, and majority of DIC will be in the form of CO_2 dissolved mode.

Benefits

- Benefits to Sequestration Program

Provide inexpensive means for measuring Dissolved Inorganic Carbons (DIC) in underground brine water *in situ,* at *higher sensitivity and at higher frequency for long period of time.*

- Benefits to CCS implementation worldwide

This will aid the Monitoring, Verification and Accounting (MVA) of CO2 sequestration